# Exact reconstruction with directional wavelets on the sphere

Y. Wiaux,[1]* J. D. McEwen,[2]* P. Vandergheynst[1]* and O. Blanc[1]

[1]*Institute of Electrical Engineering, Ecole Polytechnique Fédérale de Lausanne (EPFL), CH-1015 Lausanne, Switzerland*
[2]*Astrophysics Group, Cavendish Laboratory, University of Cambridge, Cambridge CB3 0HE*

**ABSTRACT**

A new formalism is derived for the analysis and exact reconstruction of band-limited signals on the sphere with directional wavelets. It represents an evolution of a previously developed wavelet formalism developed by Antoine & Vandergheynst and Wiaux et al. The translations of the wavelets at any point on the sphere and their proper rotations are still defined through the continuous three-dimensional rotations. The dilations of the wavelets are directly defined in harmonic space through a new kernel dilation, which is a modification of an existing harmonic dilation. A family of factorized steerable functions with compact harmonic support which are suitable for this kernel dilation are first identified. A scale-discretized wavelet formalism is then derived, relying on this dilation. The discrete nature of the analysis scales allows the exact reconstruction of band-limited signals. A corresponding exact multi-resolution algorithm is finally described and an implementation is tested. The formalism is of interest notably for the denoising or the deconvolution of signals on the sphere with a sparse expansion in wavelets. In astrophysics, it finds a particular application for the identification of localized directional features in the cosmic microwave background data, such as the imprint of topological defects, in particular, cosmic strings, and for their reconstruction after separation from the other signal components.

**Key words:** methods: data analysis – techniques: image processing – cosmic microwave background.

## 1 INTRODUCTION

Very generically, the scale-space analysis of a signal with wavelets on a given manifold defines wavelet coefficients which characterize the signal around each point of the manifold and at various scales (Mallat 1998; Antoine et al. 2004; Antoine & Vandergheynst 2007). Wavelet techniques find numerous applications in astrophysics (Starck & Murtagh 2006a). It commonly concerns the analysis of data distributed on the real line of time, or images on the plane. However, other experiments also acquire data in all directions of the sky. This is notably the case of observations of the cosmic microwave background (CMB) radiation, such as the current *Wilkinson Microwave Anisotropy Probe* (*WMAP*) satellite experiment, or the forthcoming *Planck Surveyor* satellite experiment. Sky surveys such as the NRAO Very Large Array Sky Survey (NVSS) also map data on a large fraction the celestial sphere. The scale-space analysis of such data sets requires wavelet techniques on the sphere. Various wavelet formalisms have been proposed to date (Freeden & Windheuser 1996; Holschneider 1996; Antoine & Vandergheynst 1998, 1999; Freeden et al. 1998; Narcowich et al.

2005; McEwen et al. 2006). The formalism originated by Antoine & Vandergheynst (1999) in a group-theoretic context triggered various developments (Antoine et al. 2002; Demanet & Vandergheynst 2003; Bogdanova et al. 2005), and was reconsidered in a more practical context by Wiaux et al. (2005). This approach notably found a recent and very interesting application in the analysis of the CMB data, as reviewed by McEwen et al. (2007b).

In particular, the denoising or the deconvolution of data represents a large field of application of wavelet techniques. Experimental data sets are indeed always affected by various noise sources, notably related to the instrumentation. The data can also be blurred by experimental beams associated with the instrumentation. Signals detected can also originate from different physical sources, which need to be separated. In that component separation perspective, each component can in turn be technically understood as a signal, while the other components are seen as noise. As an example, observed CMB data represent a superposition of the CMB signal itself with instrumental noise and foreground emissions, blurred by the experimental beam at each detection frequency. The denoising and the deconvolution of the signal, and the separation of its astrophysical components are of major interest for astrophysics and cosmology.

Signals with features defined at specific positions and scales typically have a sparse expansion in terms of wavelets. For such signals,

*E-mail: yves.wiaux@epfl.ch (YW); mcewen@mrao.cam.ac.uk (JDMcE); pierre.vandergheynst@epfl.ch (PV)

denoising and deconvolution algorithms are generically much more efficient when applied to the wavelet coefficients (Mallat 1998; Daubechies et al. 2004). However this requires a scheme allowing the exact reconstruction of the signals analysed from their wavelet coefficients. Moreover, localized characteristics can be elongated, in which case directional wavelets are essential. The identification and the reconstruction of localized directional features in CMB data represents a very interesting application of such a framework. It typically concerns the imprint of topological defects such as textures or cosmic strings (Kaiser & Stebbins 1984; Turok & Spergel 1990; Vilenkin & Shellard 1994; Hindmarsh & Kibble 1995). This application can be recast in a component separation approach where all continuous and typically Gaussian emissions are seen as noise, in contrast with localized directional features. Let us also emphasize that such a framework can have many applications well beyond astrophysics, from geophysics to biomedical imaging, or computer vision.

At present, the simultaneous combination of the properties of exact reconstruction and directionality is lacking in the existing wavelet formalisms on the sphere. It has only been considered for the wavelet analysis of signals on the plane (Simoncelli et al. 1992; Vandergheynst & Gobbers 2002). The primary aim of this work resides in the development of a new scale-discretized wavelet formalism for the analysis and exact reconstruction of band-limited signals on the sphere with directional wavelets. As a by-product, a new continuous wavelet formalism is also obtained, which allows the analysis of signals with a new family of wavelets relative to existing formalisms. However, the continuous range of scales required for the analysis prevents exact reconstruction in practice, for which the scale-discretized wavelet formalism proposed is essential.

The remainder of this paper is organized as follows. In Section 2, we present an existing scheme for the definition of a continuous wavelet formalism on the sphere from a generic dilation operation. We consider directional and axisymmetric wavelets and discuss the cases of the stereographic and harmonic dilations. In Section 3, we propose a new kernel dilation. A corresponding family of factorized steerable functions with compact harmonic support are identified. We show that localization and directionality properties of such functions can be controlled through kernel dilation. In Section 4, we derive a new continuous wavelet formalism from the kernel dilation with continuous scales. We then derive a new scale-discretized wavelet formalism that allows the exact reconstruction of band-limited signals in practice. We design explicitly an example wavelet. We finally recast the scale-discretized wavelet formalism in an invertible filter bank approach. In Section 5, we describe an exact algorithm accounting for the multi-resolution properties of the formalism. The memory and computation time requirements are discussed and an implementation is tested. In Section 6, we discuss the application of the formalism to the detection of cosmic strings through the denoising of full-sky CMB data. We finally conclude in Section 7.

## 2 WAVELETS FROM A GENERIC DILATION

In this section, we discuss an existing scheme for the definition of a continuous wavelet formalism on the sphere from a generic dilation operation. We consider directional and axisymmetric wavelets explicitly. We finally discuss in detail the stereographic and harmonic dilations.

### 2.1 Directional wavelets

In the continuous framework developed by Antoine & Vandergheynst (1999) and Wiaux et al. (2005), the wavelet analysis of a signal on the sphere, that is, the unit sphere $S^2$, defines wavelet coefficients through the correlation of the signal with dilated versions of a local analysis function. Theoretically, the signal can be recovered explicitly from its wavelet coefficients, provided that the local analysis functions satisfy some admissibility condition, raising it to the rank of a wavelet.

The real and harmonic structures of $S^2$ are summarized concisely as follows. We consider a three-dimensional Cartesian coordinate system $(o, o\hat{x}, o\hat{y}, o\hat{z})$ centred on the sphere, and where the direction $o\hat{z}$ identifies the North Pole. Any point $\omega$ on the sphere is identified by its corresponding spherical coordinates $(\theta, \varphi)$, where $\theta \in [0, \pi]$ stands for the colatitude, or polar angle, and $\varphi \in [0, 2\pi)$ for the longitude, or azimuthal angle. Let the continuous signal $F(\omega)$ and the local analysis function $\Psi(\omega)$ be square-integrable functions on the sphere: $F, \Psi \in L^2(S^2, d\Omega)$, with the invariant measure $d\Omega = d\cos\theta \, d\varphi$. The spherical harmonics form an orthonormal basis for the decomposition of square-integrable functions. They are explicitly given in a factorized form in terms of the associated Legendre polynomials $P_l^m(\cos\theta)$ and the complex exponentials $e^{im\varphi}$ as

$$Y_{lm}(\theta, \varphi) = \left[ \frac{2l+1}{4\pi} \frac{(l-m)!}{(l+m)!} \right]^{1/2} P_l^m(\cos\theta) \, e^{im\varphi}, \qquad (1)$$

with $l \in \mathbb{N}$, $m \in \mathbb{Z}$, and $|m| \leq l$ (Abramowitz & Stegun 1965; Varshalovich et al. 1989). The index $l$ represents an overall frequency on the sphere. The absolute value $|m|$ represents the frequency associated with the azimuthal variable $\varphi$. Any function $G \in L^2(S^2, d\Omega)$ is thus uniquely given as a linear combination of scalar spherical harmonics: $G(\omega) = \sum_{l \in \mathbb{N}} \sum_{|m| \leq l} \widehat{G}_{lm} Y_{lm}(\omega)$. This combination defines the inverse spherical harmonic transform on $S^2$. The corresponding spherical harmonic coefficients are given by the projection $\widehat{G}_{lm} = \langle Y_{lm} | G \rangle$, with $|m| \leq l$, where the bracket $\langle F_2 | F_1 \rangle = \int_{S^2} d\Omega \, F_2^*(\omega) F_1(\omega)$ generically denotes the scalar product for $F_1, F_2 \in L^2(S^2, d\Omega)$. This projection defines the direct spherical harmonic transform on $S^2$.

Continuous affine transformations such as translations, rotations, and dilations are applied to the analysis function. The continuous translations by $\omega_0 = (\theta_0, \varphi_0) \in S^2$ and rotations by $\chi \in [0, 2\pi)$ are defined by the three Euler angles defining an element $\rho = (\varphi_0, \theta_0, \chi)$ of the group of rotations in three dimensions SO(3). The operator $R(\omega_0)$ in $L^2(S^2, d\Omega)$ for the translation of amplitude $\omega_0 = (\theta_0, \varphi_0)$ of a function $G$ reads as

$$G_{\omega_0}(\omega) = [R(\omega_0) G](\omega) = G\left(R_{\omega_0}^{-1}\omega\right), \qquad (2)$$

where $R_{\omega_0}(\theta, \varphi) = [R_{\varphi_0}^{\hat{z}} R_{\theta_0}^{\hat{y}}](\theta, \varphi)$ is defined by the three-dimensional rotation matrices $R_{\theta_0}^{\hat{y}}$ and $R_{\varphi_0}^{\hat{z}}$, acting on the Cartesian coordinates $(x,y,z)$ associated with $\omega = (\theta, \varphi)$. The rotation operator $R^{\hat{z}}(\chi)$ in $L^2(S^2, d\Omega)$ for the rotation of the function $G$ around itself, by an angle $\chi \in [0, 2\pi)$, is given as

$$G_\chi(\omega) = [R^{\hat{z}}(\chi) G](\omega) = G\left(R_\chi^{\hat{z}^{-1}}\omega\right), \qquad (3)$$

where $R_\chi^{\hat{z}}(\theta, \varphi) = (\theta, \varphi + \chi)$ also follows from the action of the three-dimensional rotation matrix $R_\chi^{\hat{z}}$ on the Cartesian coordinates $(x,y,z)$ associated with $\omega = (\theta, \varphi)$. The operator incorporating both the translations and rotations simply reads as $R(\rho) = R(\omega_0)R^{\hat{z}}(\chi)$ and $G_\rho(\omega) = [R(\rho)G](\omega) = G(R_\rho^{-1}\omega)$, with $R_\rho = R_{\omega_0} R_\chi^{\hat{z}}$. The continuous dilations affect by definition the continuous scale of the function. The notion of scale may a priori be defined both in real

and in harmonic spaces on $S^2$. In the remainder of this section, we simply denote the dilated function as $G_a(\omega)$, where $a \in \mathbb{R}_+^*$ stands for a continuous dilation factor. We explicitly discuss two possible definitions of dilations in Sections 2.3 and 2.4.

The analysis of the signal $F$ with an analysis function $\Psi$ defines wavelet coefficients through the directional correlation of $F$ with the dilated functions $\Psi_a$, that is, the scalar products

$$W_\Psi^F(\rho, a) = \langle \Psi_{\rho,a} | F \rangle. \tag{4}$$

At each scale $a$, the wavelet coefficients $W_\Psi^F(\rho, a)$ therefore identify a square-integrable function on the rotation group in three dimensions SO(3). They characterize the signal around each point $\omega_0$, and in each orientation $\chi$. This defines the scale-space nature of the wavelet decomposition on the sphere.

The real and harmonic structures of the rotation group in three dimensions SO(3) are summarized concisely as follows. As discussed, any rotation $\rho$ on SO(3) is given in terms of the three Euler angles $\rho = (\varphi, \theta, \chi)$, with $\theta \in [0, \pi]$, and $\varphi, \chi \in [0, 2\pi)$. Let $H(\rho)$ be a square-integrable function on SO(3): $H \in L^2(SO(3), d\rho)$, with the invariant measure $d\rho = d\varphi d\cos\theta d\chi$. The Wigner $D$-functions are the matrix elements of the irreducible unitary representations of weight $l$ of the group in $L^2(SO(3), d\rho)$. By the Peter–Weyl theorem on compact groups, the matrix elements $D_{mn}^{l*}$ also form an orthogonal basis in $L^2(SO(3), d\rho)$. They are explicitly given in a factorized form in terms of the real Wigner $d$-functions $d_{mn}^l(\theta)$ and the complex exponentials, $e^{-im\varphi}$ and $e^{-in\chi}$, as

$$D_{mn}^l(\varphi, \theta, \chi) = e^{-im\varphi} d_{mn}^l(\theta) e^{-in\chi}, \tag{5}$$

with $l \in \mathbb{N}$, $m, n \in \mathbb{Z}$, and $|m|, |n| \le l$ (Varshalovich et al. 1989; Brink & Satchler 1993). Again, $l$ represents an overall frequency on SO(3), and $|m|$ and $|n|$ the frequencies associated with the variables $\varphi$ and $\chi$, respectively. Any function $H \in L^2(SO(3), d\rho)$ is thus uniquely given as a linear combination of Wigner $D$-functions: $H(\rho) = \sum_{l \in \mathbb{N}} (2l+1)/8\pi^2 \sum_{|m|, |n| \le l} \widehat{H}_{mn}^l D_{mn}^{l*}(\rho)$. This combination defines the inverse Wigner $D$-function transform on SO(3). The corresponding Wigner $D$-function coefficients are given by the projection $\widehat{H}_{mn}^l = \int_{SO(3)} d\rho\, D_{mn}^l(\rho) H(\rho)$. This projection defines the direct Wigner $D$-function transform on SO(3).

At each scale, the direct Wigner $D$-function transform of the wavelet coefficients is given as the point-wise product of the spherical harmonic coefficients of the signal and the wavelet:

$$\widehat{(W_\Psi^F)}_{mn}^l(a) = \frac{8\pi^2}{2l+1} \widehat{(\Psi_a)}_{ln}^* \widehat{F}_{lm}. \tag{6}$$

Indeed, the orthonormality of scalar spherical harmonics implies the Plancherel relation $\langle F_2 | F_1 \rangle = \sum_{l \in \mathbb{N}} \sum_{|m| \le l} \widehat{(F_2)}_{lm}^* \widehat{(F_1)}_{lm}$ for $F_1, F_2 \in L^2(S^2, d\Omega)$, and the action of the operator $R(\rho)$ on $G \in L^2(S^2, d\Omega)$ reads in terms of its spherical harmonic coefficients as $\widehat{(G_\rho)}_{lm} = \sum_{|n| \le l} D_{mn}^l(\rho) \widehat{G}_{ln}$.

The reconstruction of a signal $F$ from its wavelet coefficients with an analysis function $\Psi$ is given as

$$F(\omega) = \int_{\mathbb{R}_+^*} d\mu(a) \int_{SO(3)} d\rho\, W_\Psi^F(\rho, a) [R(\rho) L_\Psi \Psi_a](\omega). \tag{7}$$

In this relation, the scale integration measure $d\mu(a)$ is part of the definition of the dilation operation itself (see Sections 2.3 and 2.4). The operator $L_\Psi$ in $L^2(S^2, d\Omega)$ is defined by its action on the spherical harmonic coefficients of a function $G$: $\widehat{L_\Psi G}_{lm} = \widehat{G}_{lm}/C_\Psi^l$. The reconstruction formula holds if and only if the analysis function satisfies the following admissibility condition for all $l \in \mathbb{N}$:

$$0 < C_\Psi^l = \frac{8\pi^2}{2l+1} \sum_{|m| \le l} \int_{\mathbb{R}_+^*} d\mu(a)\, |\widehat{(\Psi_a)}_{lm}|^2 < \infty. \tag{8}$$

In this case, the analysis function $\Psi$ is by definition raised to the rank of a wavelet. From relation (8), the admissibility condition intuitively requires that the whole wavelet family $\{\Psi_a(\omega)\}$, for $a \in \mathbb{R}_+^*$, covers each frequency index $l$ with a finite and non-zero amplitude, hence preserving the signal information at each frequency. Note that a direct connection exists between the generic relations (7) and (8) for the signal reconstruction, and the theory of frames on the sphere (Bogdanova et al. 2005).

We generally consider band-limited signals. Any function $G \in L^2(S^2, d\Omega)$ is said to be band-limited with the band limit $B$, for any $B \in \mathbb{N}^0$, if $\widehat{G}_{lm} = 0$ for all $l, m$ with $l \ge B$. Any function $H \in L^2(SO(3), d\rho)$ is said to be band-limited with the band limit $B$, for any $B \in \mathbb{N}^0$, if $\widehat{H}_{mn}^l = 0$ for all $l, m, n$ with $l \ge B$. From relation (6), if the signal $F$ or the wavelet $\Psi$ are band-limited on $S^2$, then the wavelet coefficients $W_\Psi^F$ are automatically band-limited on SO(3), with the same band limit $B$.

Let us already notice that the reconstruction is ensured theoretically from relation (7), through the integration on the continuous parameter $\rho \in SO(3)$ for translations and rotations of the wavelet, and on the continuous dilation factor $a \in \mathbb{R}_+^*$. However, in practice, the reconstruction would require the definition of exact quadrature rules for the numerical integrations. Exact quadrature rules for integration of band-limited signals on $S^2$ exist on equiangular (Driscoll & Healy 1994) and Gauss–Legendre (Doroshkevich et al. 2005a,b) pixelizations of $(\theta_0, \varphi_0)$. HEALPIX pixelizations (Górski et al. 2005)[1] of $(\theta_0, \varphi_0)$ on $S^2$ provide approximate quadrature rules which can also be made very precise, thanks to an iteration process. Pixelizations may, for instance, be defined on SO(3) by combining pixelizations on $S^2$ with an equiangular sampling of $\chi$. Corresponding quadrature rules can be made exact on the pixelizations based on equiangular and Gauss–Legendre pixelizations on $S^2$, while those based on HEALPIX pixelizations are approximate. This extension basically relies on the separation of the integration variables (Maslen & Rockmore 1997a,b; Kostelec & Rockmore 2003) from relation (5).

However, exact quadrature rules do not exist for the integration over scales $a \in \mathbb{R}_+^*$. In practice, this prevents an exact reconstruction of the signal analysed. A scheme allowing an exact reconstruction requires a discretization of the dilation factor. A scale-discretized wavelet formalism is proposed in Section 4, thanks to a specific choice of dilation, and through an integration of the dilation factor by slices in relation (7).

## 2.2 Axisymmetric wavelets

Any general function $G \in L^2(S^2, d\Omega)$ explicitly dependent on the azimuthal angle $\varphi$, is said to be directional: $G = G(\theta, \varphi)$. By opposition, any function $A \in L^2(S^2, d\Omega)$ independent of the azimuthal angle $\varphi$ is said to be zonal, or axisymmetric: $A = A(\theta)$. It only exhibits non-zero spherical harmonic coefficients for $m = 0$: $\widehat{A}_{lm} = \widehat{A}_{l0}\delta_{m0}$.

In this particular case, the directional correlation of a signal $F$ with $A$ reduces to a standard correlation obviously independent of the rotation angle $\chi$ (Wiaux et al. 2006). The analysis of $F$ with an axisymmetric analysis function $A$ defines wavelet coefficients through the standard correlation of $F$ with the dilated functions $A_a$, that is, the scalar products

$$W_A^F(\omega_0, a) = \langle A_{\omega_0,a} | F \rangle. \tag{9}$$

---

[1] http://healpix.jpl.nasa.gov/

At each scale $a$, the wavelet coefficients identify a square-integrable function on $S^2$ rather than on SO(3). The spherical harmonic transform of the wavelet coefficients is still given as the point-wise product of the spherical harmonic coefficients of the signal and the wavelet:

$$\widehat{\left(W_A^F\right)}_{lm}(a) = \sqrt{\frac{4\pi}{2l+1}} \widehat{(A_a)}_{l0}^* \widehat{F}_{lm}. \tag{10}$$

This relation simply follows from relation (6) and the equality $D_{m0}^l(\omega, 0) = [4\pi/(2l+1)]^{1/2} Y_{lm}^*(\omega)$.

The reconstruction of $F$ from its wavelet coefficients reads as

$$F(\omega) = \int_{\mathbb{R}_+^*} d\mu(a) \int_{S^2} d\omega_0 W_A^F(\omega_0, a) \left[R(\omega_0) L_A A_a\right](\omega), \tag{11}$$

for any scale integration measure $d\mu(a)$, and with the operator $L_A$ in $L^2(S^2, d\Omega)$ defined by $\widehat{L_A G}_{l0} = \widehat{G}_{l0}/C_A^l$. The reconstruction formula holds if and only if the analysis function satisfies the following admissibility condition for all $l \in \mathbb{N}$:

$$0 < C_A^l = \frac{4\pi}{2l+1} \int_{\mathbb{R}_+^*} d\mu(a) \, |\widehat{(A_a)}_{l0}|^2 < \infty. \tag{12}$$

### 2.3 Stereographic dilation

In the original set up proposed by Antoine & Vandergheynst (1999), the stereographic dilation of functions is considered, which is explicitly defined in real space on $S^2$. The stereographic dilation operator $D(a)$ on $G \in L^2(S^2, d\Omega)$, for a continuous dilation factor $a \in \mathbb{R}_+^*$, is defined in terms of the inverse of the corresponding stereographic dilation $D_a$ on points in $S^2$. It reads as

$$G_a(\omega) = [D(a) G](\omega)$$
$$= \lambda^{1/2}(a, \theta) G\left(D_a^{-1}\omega\right), \tag{13}$$

with $\lambda^{1/2}(a, \theta) = a^{-1}[1 + \tan^2(\theta/2)]/[1 + a^{-2}\tan^2(\theta/2)]$. The dilated point is given by $D_a(\theta, \varphi) = (\theta_a(\theta), \varphi)$ with the linear relation $\tan(\theta_a(\theta)/2) = a \tan(\theta/2)$. The dilation operator therefore maps the sphere without its South Pole on itself: $\theta_a(\theta) : \theta \in [0, \pi) \rightarrow \theta_a \in [0, \pi)$. This dilation operator is uniquely defined by the requirement of the following natural properties. The dilation of points on $S^2$ must be a radial (i.e. only affecting the radial variable $\theta$ independently of $\varphi$, and leaving $\varphi$ invariant) and conformal (i.e. preserving the measure of angles in the tangent plane at each point) diffeomorphism (i.e. a continuously differentiable bijection). The normalization by $\lambda^{1/2}(a, \theta)$ in equation (13) is uniquely determined by the requirement that the dilation of functions in $L^2(S^2, d\Omega)$ be a unitary operator (i.e. preserving the scalar product in $L^2(S^2, d\Omega)$, and specifically the norm of functions). Note that the stereographic dilation operation is supported by a group structure for the composition law of the corresponding operator $D(a)$. A group homomorphism also holds with the operation of multiplication by $a$ on $\mathbb{R}_+^*$.

In this setting, the effect of the dilation on the spherical harmonic coefficients of the dilated function is not easily tractable analytically. Consequently, the admissibility condition (8) is difficult to check in practice. On the contrary, wavelets on the plane are well known, and may be easily constructed, as the corresponding admissibility condition reduces to a zero mean condition for a function both integrable and square-integrable. In that context, a correspondence principle was proved (Wiaux et al. 2005), stating that the inverse stereographic projection of a wavelet on the plane leads to a wavelet on the sphere. This correspondence principle notably requires the definition of a scale integration measure identical to the measure used on the plane: $d\mu(a) = a^{-3}da$. Note that this measure naturally appears in the original group-theoretic context (Antoine & Vandergheynst 1999).

### 2.4 Harmonic dilation

Another possible definition of the dilation of functions may be considered, which is explicitly defined in harmonic space on $S^2$. It was proposed in previous developments relative to the definition of a wavelet formalism on the sphere (Holschneider 1996; McEwen et al. 2006). The harmonic dilation is defined directly on $G \in L^2(S^2, d\Omega)$ through a sequence of prescriptions rather than in terms of the application of an simple operator. First, an arbitrary prescription must be chosen to define a set of generating functions $\tilde{G}_m(k)$ of a continuous variable $k \in \mathbb{R}_+$, for each $m \in \mathbb{Z}$. These functions are identified to the spherical harmonic coefficients of $G$ through: $\tilde{G}_m(l) = \widehat{G}_{lm}$ for $l \in \mathbb{N}$, and $|m| \leq l$. Secondly, the variable $k$ is dilated linearly, $k = l \rightarrow k = a \, l$, just as would be the norm of the Fourier frequency on the plane. For a continuous dilation factor $a \in \mathbb{R}_+^*$, the spherical harmonic coefficients of the dilated function $G_a$ are defined by

$$\widehat{(G_a)}_{lm} = \tilde{G}_m(al). \tag{14}$$

In the corresponding continuous wavelet formalism, the analysis function $\Psi$ must satisfy the following form of the admissibility condition (8). On the one hand, $\widehat{\Psi}_{00} = \tilde{\Psi}_0(0) = 0$, which corresponds to the requirement that $\Psi$ has a zero mean on the sphere:

$$\frac{1}{4\pi} \int_{S^2} d\Omega \, \Psi(\omega) = 0. \tag{15}$$

This zero mean is of course preserved through harmonic dilation. As the zero frequency is not supported by the wavelets, only signals with zero mean can be analysed in this formalism (see relation 6). Let us remark that wavelets on the sphere dilated through the stereographic dilation do not necessarily have a zero mean. On the other hand, the scale integration measure can arbitrarily be chosen as $d\mu(a) = a^{-1}da$. This leads to a simple expression of the remaining constraints for $l \in \mathbb{N}^0$ as

$$0 < C_\Psi^l = \frac{8\pi^2}{2l+1} \sum_{|m| \leq l} \int_{\mathbb{R}_+} \frac{dk'}{k'} |\tilde{\Psi}_m(k')|^2 < \infty. \tag{16}$$

The left-hand side inequality implies $0 < \int_{\mathbb{R}_+} dk'/k' |\tilde{\Psi}_{m_0}(k')|^2$ for at least one of the first two generating functions: $m_0 \in \{0, 1\}$. In other words, either $\tilde{\Psi}_0$ or $\tilde{\Psi}_1$ must be non-zero on a set of non-zero measure on $\mathbb{R}_+$. The right-hand side inequality implies $\int_{\mathbb{R}_+} dk'/k' |\tilde{\Psi}_m(k')|^2 < \infty$ for all generating functions: $m \in \mathbb{Z}$. Hence, the generating functions must satisfy $\tilde{\Psi}_m(0) = 0$ [this condition encompasses the zero mean condition (15) in the form $\tilde{\Psi}_0(0) = 0$] and tend to zero when $k' \rightarrow \infty$. With this choice of scale integration measure, the constraints summarize to the requirement that each generating function satisfies a condition very similar to the wavelet admissibility condition for an axisymmetric wavelet on the plane (Antoine et al. 2004)[2] defined by a Fourier transform identical to $\tilde{\Psi}_m(k)$. Consequently, the wavelet admissibility condition (16) can be checked in practice and wavelets associated with the harmonic dilation can be designed easily.

---

[2] The exact wavelet admissibility condition on the plane reduces to a zero mean condition for functions that are both integrable and square-integrable.

For continuous axisymmetric wavelets, a unique generating function $\tilde{A}_0(k)$ of a continuous variable $k \in \mathbb{R}_+$ is required. The admissibility condition (12) reduces to the following expression. The analysis function $A$ must have a zero mean and only allows the analysis of signals with zero mean. A unique additional condition holds independently of $l$:

$$0 < C_A = \int_{\mathbb{R}_+} \frac{dk'}{k'} |\tilde{A}_0(k')|^2 < \infty. \tag{17}$$

This condition actually encompasses the zero mean condition in the form $\tilde{A}_0(0) = 0$, and also requires that the generating function must tend to zero when $k' \to \infty$. The coefficients entering the reconstruction formula (11) read as $C_A^l = 4\pi C_A/(2l+1)$, for $l \in \mathbb{N}^0$.

## 2.5 Discussion

On the one hand, the harmonic dilation lacks some of the important properties which hold under stereographic dilation. As the harmonic dilation does not act on points, the question of the corresponding properties of a radial and conformal diffeomorphism make no sense. The harmonic dilation of functions is not either a unitary procedure. It does not preserve the scalar product in $L^2(S^2, d\Omega)$, or specifically the norm of functions. This is due to the requirement of definition of generating functions for any function to be dilated. A group structure for the composition of harmonic dilations holds only if successive dilations of a function $G$ are defined through linear dilation of the variable $k$ of a unique generating function $\tilde{G}_m(k)$ for each $m \in \mathbb{Z}$. The same condition applies to the existence of a corresponding homomorphism structure with the operation of multiplication by $a$ on $\mathbb{R}_+^*$.

Moreover, the harmonic dilation is explicitly defined in harmonic space. The evolution in real space of localization and directionality properties of functions on the sphere through harmonic dilation is therefore not known analytically. However, in the Euclidean limit where a function is localized on a small portion of the sphere, this portion is assimilated to the tangent plane, and the stereographic and harmonic dilations both identify with the standard dilation in the plane. For each $m \in \mathbb{Z}$, the overall frequency index $l \in \mathbb{N} \to \infty$ identifies with the continuous variable $k \in \mathbb{R}_+ \to \infty$, corresponding to the norm of the Fourier frequency on the plane (Holschneider 1996). Thus, in particular, the evolution of localization properties of functions through harmonic dilation is at least controlled in the Euclidean limit.

On the other hand, the very simple action of the harmonic dilation in harmonic space also exhibits several advantages relative to the stereographic dilation. Notably, the harmonic dilation ensures that the band limit of a wavelet and of the corresponding wavelet coefficients, is reduced by a factor $a$. Such a multi-resolution property is essential in reducing the memory and computation time requirements for the wavelet analysis of signals. It does not hold under stereographic dilation. Moreover, as already emphasized, a scheme allowing an exact reconstruction of signals from their wavelet coefficients requires a discretization of the dilation factor. The definition of a scale-discretized wavelet formalism through an integration of the dilation factor $a$ by slices in the continuous wavelet formalism turns out to be very natural with a dilation defined in harmonic space, but not with the stereographic dilation. Indeed, one would like the dilation operation acting on scale-discretized functions after the integration of the dilation factor by slices to be the same as the original dilation operation. It will become obvious that this property holds for a dilation defined in harmonic space, but not for the stereographic dilation.

In conclusion, no obvious definition of dilation is imposed for the development of a wavelet formalism on the sphere. However, considering our aim for a scale-discretized wavelet formalism, as well as the essential criterion of defining a formalism with multi-resolution properties, we will focus on a scale-discretized wavelet formalism from a dilation defined in harmonic space. However, for any dilation defined in harmonic space, the evolution of the localization and directionality properties of functions in real space through dilation needs to be understood and controlled. In that regard, we amend the harmonic dilation (14) and define a kernel dilation to be applied on functions which are said to be factorized steerable functions with compact harmonic support. Moreover, the kernel dilation will also render the transition between the continuous and scale-discretized formalism much simpler and more transparent than what the harmonic dilation can provide.

## 3 KERNEL DILATION

In this section, we define the kernel dilation on factorized functions in harmonic space on the sphere. We consider, in particular, factorized steerable functions with compact harmonic support. We also study the localization and directionality properties in real space for such functions, as well as the controlled evolution of these properties through kernel dilation.

### 3.1 Factorized functions and kernel dilation

A function $G \in L^2(S^2, d\Omega)$ can be defined to be a factorized function in harmonic space if it can be written in the form:

$$\widehat{G}_{lm} = \tilde{K}_G(l) S_{lm}^G, \tag{18}$$

for $l \in \mathbb{N}$, and $|m| \leq l$. The positive real *kernel* $\tilde{K}_G(k) \in \mathbb{R}_+$ is a generating function of a continuous variable $k \in \mathbb{R}_+$, initially evaluated on integer values $k = l$. The directionality coefficients $S_{lm}^G$, for $l \in \mathbb{N}$, and $|m| \leq l$, define the *directional split* of the function. In particular, for a real function $G$, they bear the same symmetry relation as the spherical harmonic coefficients $\widehat{G}_{lm}$ themselves: $S_{lm}^{G*} = (-1)^m S_{l(-m)}^G$. Without loss of generality, one can impose

$$\sum_{|m| \leq l} |S_{lm}^G|^2 = 1, \tag{19}$$

for the values of $l$ for which $S_{lm}^G$ is non-zero for at least one value of $m$. Hence, localization properties of a function $G$, such as a measure of dispersion of angular distances around its central position as weighted by the function values, are governed by the kernel and to a lesser extent by the directional split. Indeed, the power contained in the function $G$ at each allowed value of $l$ is fixed by the kernel only. The norm of $G \in L^2(S^2, d\Omega)$ reads as $||G||^2 = \sum_{l \in \mathbb{N}} \tilde{K}_G^2(l)$, where the sum runs over the values of $l$ for which $S_{lm}^G$ is non-zero for at least one value of $m$. However, the directional split is essential in defining the directionality properties measuring the behaviour of the function with the azimuthal variable $\varphi$, because of it bears the entire dependence of the spherical harmonic coefficients of the function in the index $m$.

The kernel dilation applied to a factorized function (18) is simply defined by application of the harmonic dilation (14) to the kernel only. The directionality of the dilated function is defined through the same directional split as the original function. For a continuous dilation factor $a \in \mathbb{R}_+^*$, the dilated function therefore reads as

$$\widehat{(G_a)}_{lm} = \tilde{K}_G(al) S_{lm}^G. \tag{20}$$

Let us emphasize that the directionality coefficients $S_{lm}^G$ are not affected by dilations, contrary to what the complete action of the harmonic dilation (14) would imply. The kernel and harmonic dilations strictly identify with one another when applied to factorized axisymmetric functions $A$, for which the directional split takes the trivial values $S_{lm}^A = \delta_{m0}$ for $l \in \mathbb{N}$.

### 3.2 Compact harmonic support

Any function $G \in L^2(S^2, d\Omega)$ can be said to have a compact harmonic support in the interval $l \in (\lfloor \alpha^{-1}B \rfloor, B)$, for any $B \in \mathbb{N}^0$ and any real value $\alpha > 1$, if

$$\widehat{G}_{lm} = 0 \quad \text{for all} \quad l, m \quad \text{with} \quad l \notin \left( \lfloor \alpha^{-1}B \rfloor, B \right), \tag{21}$$

where $\lfloor x \rfloor$ denotes the largest integer value below $x \in \mathbb{R}$. Note that the compactness of the harmonic support of $G$ can be defined as the ratio of the band limit to the width of its support interval.

For a factorized function $G$ of the form (18), the compact harmonic support in the interval $l \in (\lfloor \alpha^{-1}B \rfloor, B)$ is ensured by the choice of a kernel with compact support in the interval $k \in (\alpha^{-1}B, B)$:

$$\tilde{K}_G(k) = 0 \quad \text{for} \quad k \notin (\alpha^{-1}B, B). \tag{22}$$

The compactness of the harmonic support of $G$ can simply be estimated from the compact support of the kernel as $c(\alpha) = \alpha/(\alpha - 1) \in [1, \infty)$. One has $c(\alpha) \to \infty$ when $\alpha \to 1$, and $c(\alpha) \to 1$ when $\alpha \to \infty$. Typical values would be $\alpha = 2$ corresponding to a compactness $c(2) = 2$, or $\alpha = 1.1$ leading to a higher compactness $c(1.1) = 11$.

By a kernel dilation with a dilation factor $a \in \mathbb{R}_+^*$ in (20), the compact support of the dilated kernel $\tilde{K}_G(ak) \in \mathbb{R}_+$ is defined in the interval $k \in (a^{-1}\alpha^{-1}B, a^{-1}B)$. The compact harmonic support of the dilated function $G_a$ itself is thus defined in the corresponding interval $l \in (\lfloor a^{-1}\alpha^{-1}B \rfloor, \lceil a^{-1}B \rceil)$, where $\lceil x \rceil$ denotes the smallest integer value above $x \in \mathbb{R}$. In particular, the compactness of the harmonic support of a function remains invariant through a kernel dilation.

### 3.3 Steerable functions

The notion of steerability was first introduced on the plane (Freeman & Adelson 1991; Simoncelli et al. 1992), and more recently defined on the sphere (Wiaux et al. 2005). By definition, $G \in L^2(S^2, d\Omega)$ is steerable if any rotation of the function around itself may be expressed as a linear combination of a finite number $M$ of basis functions $G_p$:

$$G_\chi(\omega) = \sum_{p=0}^{M-1} k_p(\chi) G_p(\omega). \tag{23}$$

The square-integrable functions $k_p(\chi)$ on the circle $S^1$, with $1 \leq m \leq M$, and $M \in \mathbb{N}^0$, are called interpolation weights. Intuitively, steerable functions have a non-zero angular width in the azimuthal angle $\varphi$, which renders them sensitive to a range of directions and enables them to satisfy the steerability relation. This non-zero angular width naturally corresponds to an azimuthal band limit $N \in \mathbb{N}^0$ in the frequency index $m$ associated with the azimuthal variable $\varphi$:

$$\widehat{G}_{lm} = 0 \quad \text{for all} \quad l, m \quad \text{with} \quad |m| \geq N. \tag{24}$$

It can actually be shown that the property of steerability (23) is equivalent to the existence of an azimuthal band limit $N$ (24).

On the one hand, if a function $G$ is steerable with $M$ basis functions, then the number $T$ of values of $m$ for which $\widehat{G}_{lm}$ has a non-zero value for at least one value of $l$ is lower or equal to $M$: $M \geq T$. This was first established for functions on the plane (Freeman & Adelson 1991), and the proof is absolutely identical on the sphere. As a consequence, the function has some azimuthal band limit $N$, with $T \leq 2N - 1$.

On the other hand, if a function $G$ has an azimuthal band limit $N$, then it is steerable, and the number of basis functions can be reduced at least to $M = 2N - 1$. This second part of the equivalence can be proved by explicitly deriving a steerability relation for band-limited functions with an azimuthal band limit $N$. Any band-limited function $G$ can, in particular, be steered using $M$ rotated versions $G_{\chi_p} = R^{\hat{z}}(\chi_p)G$ as basis functions, and interpolation weights given by simple translations by $\chi_p$ of a unique square-integrable function $k(\chi)$ on the circle $S^1$:

$$G_\chi(\omega) = \sum_{p=0}^{M-1} k(\chi - \chi_p) G_{\chi_p}(\omega), \tag{25}$$

for specific rotation angles $\chi_p$ with $0 \leq p \leq M - 1$. One may choose $M = 2N - 1$ equally spaced rotation angles $\chi_p \in [0, 2\pi)$ as $\chi_p = 2\pi p/(2N - 1)$, with $0 \leq p \leq 2N - 2$. The function $k(\chi)$ is then defined by the Fourier coefficients $\widehat{k}_m = 1/(2N - 1)$ for $|m| \leq N - 1$ and $\widehat{k}_m = 0$ otherwise. Note that the angles $\chi_p$ and the structure of the function $k(\chi)$ are independent of the explicit non-zero values $\widehat{G}_{lm}$.

Typically, if $\widehat{G}_{lm}$ has a non-zero value for at least one value of $l$ for all $m$ with $|m| \leq N - 1$, then $T = 2N - 1$ and the function is optimally steered by these $M = T$ angles and the function $k(\chi)$ described. On the contrary, when values of $m$, with $|m| \leq N - 1$, exist for which $\widehat{G}_{lm} = 0$ for all values of $l$, then $T < 2N - 1$ and one might want to reduce the number $M = 2N - 1$ of basis functions. Depending on the distribution of the $T$ values of $m$ for which $\widehat{G}_{lm}$ has a non-zero value for at least one value of $l$, the number of basis functions required to steer the band-limited function may indeed be optimized to its smallest possible value $M = T$. This optimization is notably reachable for functions with specific distributions of the $T$ values of $m$, corresponding to particular symmetries in real space. For example, a function $G$ is even or odd through rotation around itself by $\chi = \pi$ if and only if $\widehat{G}_{lm}$ has non-zero values only for, respectively, even or odd values of $m$. This property notably implies that the central position of the function $G$ identifies with the North Pole, in the sense that its modulus $|G|$ is then always even through rotation around itself by $\chi = \pi$. The combination of an azimuthal band limit $N$ with that symmetry reads as

$$\widehat{G}_{lm} = 0 \quad \text{for all} \quad l, m \quad \text{with} \quad m \notin T_N, \tag{26}$$

with

$$T_N = \{-(N-1), -(N-3), \ldots, (N-3), (N-1)\}. \tag{27}$$

In this particular case, $T = N$ and one may choose $M = N$ equally spaced rotation angles $\chi_p \in [0, \pi)$ as $\chi_p = \pi p/N$, with $0 \leq p \leq N - 1$, and steer the function through relation (25). The function $k(\chi)$ is defined by the Fourier coefficients $\widehat{k}_m = 1/N$ for $m \in T_N$ and $\widehat{k}_m = 0$ otherwise.

In summary, the property of steerability is indeed equivalent to the existence of an azimuthal band limit in $m$. For a factorized function $G$ of the form (18), steerability constraints such as (24) and (26) are ensured by the directionality coefficients $S_{lm}^G$, independently of the kernel. Consequently, any relation of steerability remains unchanged through a kernel dilation (20), which by definition only affects the kernel.

## 3.4 Localization control

Let us consider the Euclidean limit where a function is localized on a small portion of the sphere which can be assimilated to the tangent plane. As discussed, the harmonic dilation (14) identifies with the standard dilation in the plane in that limit (Holschneider 1996). Hence, for factorized steerable functions with compact harmonic support, the kernel dilation (20) certainly shares the same property if it identifies with the harmonic dilation itself in the limit $l \to \infty$. This is ensured by considering functions with directionality coefficients $S_{lm}^G$ which become independent of $l$ in the limit $l \to \infty$. Consequently, the evolution of localization properties of functions through kernel dilation is also controlled in the Euclidean limit. However, a much more important localization property holds for the kernel dilation at any frequency range for factorized functions with compact harmonic support.

A typical localization property of a function $G \in L^2(S^2, d\Omega)$ is a measure of dispersion of angular distances around its central position, as weighted by the function values. The corresponding measure in harmonic space is defined by the dispersion of the values of $l$ around their central position, as weighted by the values of the spherical harmonic coefficients $\widehat{G}_{lm}$, for each value of $m$. It is well known that the smaller the dispersion in real space, the larger the dispersion in harmonic space. An optimal Dirac delta distribution on the sphere $\delta_{S^2}(\omega)$ exhibits an infinite series in $l$ of spherical harmonic coefficients: $\widehat{(\delta_{S^2})}_{lm} = [(2l + 1)/4\pi]^{1/2} \delta_{m0}$. On the contrary a spherical harmonic $Y_{lm}$, completely non-localized in real space on $S^2$, by definition exhibits a unique frequency $l$.

In particular, we need to understand the evolution of this localization property of a factorized steerable function $G$ with compact harmonic support through the kernel dilation (20). Let us consider for simplicity a factorized axisymmetric function $A$ with compact harmonic support, for which the kernel and harmonic dilations identify with one another. For an initial compact harmonic support in the interval $l \in (\lfloor \alpha^{-1}B \rfloor, B)$, the kernel dilation by a factor $a$ modifies the interval to $l \in (\lfloor a^{-1}\alpha^{-1}B \rfloor, \lceil a^{-1}B \rceil)$. Hence, in harmonic space the width of the harmonic support interval is multiplied by $a^{-1}$. This also measures the evolution of the dispersion in harmonic space. In real space, one can intuitively consider that the corresponding dispersion of the values of the angular distance $\theta$ around the North Pole (which is the central position of any axisymmetric function) is multiplied by $a$. This intuition is actually only exact in the Euclidean limit $l \to \infty$, reached when $a \to 0$. However, a weaker property holds though, on a wide class of axisymmetric functions on the sphere, in particular on factorized axisymmetric functions with compact harmonic support. It takes the form of the following upper bound through the kernel dilation by $a$ of such an axisymmetric function $A$ at a given angular distance $\theta$ from the North Pole:

$$|A_a(\theta)| \leq b_{(A,k)} \frac{a^{-2}}{1 + (\theta/a)^k}, \tag{28}$$

for any integer $k \geq 2$ and for some constant $b_{(A,k)}$ depending on $A$ and $k$ (Narcowich et al. 2005). The ratio of the bounds at the North Pole and at any fixed angular distance $\theta$ simply reads as $1 + (\theta/a)^k$. When $a$ increases, this ratio gets closer to unity and the bound is less constraining, enabling a larger dispersion of the values of the angular distance $\theta$ around the North Pole. When $a$ decreases, the ratio increases and the bound is more constraining, hence imposing a smaller dispersion of the values of the angular distance $\theta$ around the North Pole. This ensures a good behaviour in real space for the

kernel dilation, when applied to factorized axisymmetric functions with compact harmonic support.

In summary, the dispersion of angular distances around the central position of a function $G$ defines a localization property. We have shown that the evolution of the localization of factorized axisymmetric functions with compact harmonic support through kernel dilation is controlled by the bound (28). For completeness, the corresponding bound should be analysed for the kernel dilation of factorized steerable functions with compact harmonic support, but this goes beyond the scope of this work. The verification of more detailed localization properties in real space for a function designed from its spherical harmonic coefficients requires a numerical evaluation of sampled values of that function.

## 3.5 Directionality control

Let us consider a typical directionality property of a function $G \in L^2(S^2, d\Omega)$, such as measured by its auto-correlation function. The auto-correlation function of $G$ is defined as the scalar product between two rotated versions of the function around itself by angles $\chi, \chi' \in [0, 2\pi)$. This auto-correlation only depends on the difference of the rotation angles $\Delta\chi = \chi - \chi'$ and is therefore considered in the space $L^2(S^1, d\chi)$ of square-integrable functions on the circle $S^1$ : $C^G(\Delta\chi) = \langle G_\chi | G_{\chi'} \rangle$. The peakedness of the auto-correlation function in $\Delta\chi$ can be considered as a measure of the directionality of the function: the more peaked the auto-correlation, the more directional the function (Wiaux et al. 2005). From the Plancherel relation $\langle F_2 | F_1 \rangle = \sum_{l \in \mathbb{N}} \sum_{|m| \leq l} \widehat{(F_2)}_{lm}^* \widehat{(F_1)}_{lm}$ for $F_1$, $F_2 \in L^2(S^2, d\Omega)$, and the expression $\widehat{(G_\chi)}_{lm} = e^{-im\chi} \widehat{G}_{lm}$ for the action of the operator $R^{\hat{z}}(\chi)$ on $G$, one gets

$$C^G(\Delta\chi) = \sum_{l \in \mathbb{N}} \sum_{|m| \leq l} e^{-im\Delta\chi} |\widehat{G}_{lm}|^2. \tag{29}$$

The value of the auto-correlation function at $\Delta\chi = 0$ obviously defines the square of the norm of the function : $C^G(0) = ||G||^2$.

For a factorized function (18), the auto-correlation function is strongly related to the directional split. Let us also recall that in the case of a steerable function $G$ defined through (25), the interpolation weights depend on the values of $m$ for which the spherical harmonic coefficients have non-zero values and on the rotation angles $\chi_p$, but not on the values $\widehat{G}_{lm}$ themselves. This leaves enough freedom to design a suitable auto-correlation function and thus control the directionality of the function. Let us also consider a compact harmonic support (21) in the interval $(\lfloor \alpha^{-1}B \rfloor, B)$. We analyse the particular case where the directionality coefficients are independent of $l$ for $l \geq N - 1$,

$$S_{lm}^G = S_{(N-1)m}^G \quad \text{for all} \quad l, m \quad \text{with} \quad l \geq N - 1, \tag{30}$$

and where $N - 1$ is lower or equal to the lowest integer value above the lower bound of the compact harmonic support interval, that is, $N - 1 \leq \lfloor \alpha^{-1}B \rfloor + 1$. In that limit, the auto-correlation reads as

$$C^G(\Delta\chi) = ||G||^2 \sum_{|m| \leq N-1} e^{-im\Delta\chi} |S_{(N-1)m}^G|^2. \tag{31}$$

In other words, the square of the complex norm of the directionality coefficients identifies with the Fourier coefficients of $C^G(\Delta\chi)$ in $L^2(S^1, d\chi)$. Note that a better directionality of a steerable function, as measured by its auto-correlation function, is inevitably associated with a larger band limit $N$, and with a larger number $T$ of values of $m$ for which $\widehat{G}_{lm}$ has a non-zero value for at least one value of $l$. Indeed, on the circle $S^1$ as on the plane or the sphere, the smaller

the dispersion of $\Delta\chi$ in real space, the larger the dispersion of $m$ in harmonic space. Consequently, a better directionality of a steerable function requires an increased number $M$ of basis functions.

We need to understand the evolution of this directionality property of a factorized steerable function $G$ with compact harmonic support through the kernel dilation (20). The correlation function of two dilated versions $G_a$ and $G_{a'}$ by factors $a$ and $a'$ in $\mathbb{R}_+^*$ is defined through the scalar product $C_{aa'}^G(\Delta\chi) = \langle G_{\chi,a}|G_{\chi',a'}\rangle$. We consider again the case where the directionality coefficients are independent of $l$ for $l \geq N - 1$ and where the azimuthal band limit for steerability is lower than the lower bound of the compact harmonic support of each of the two dilated versions of $G$: $N - 1 \leq \lfloor a^{-1}\alpha^{-1}B \rfloor + 1$ and $N - 1 \leq \lfloor a'^{-1}\alpha^{-1}B \rfloor + 1$. In that limit, the correlation $C_{aa'}^G(\Delta\chi)$ reads as

$$C_{aa'}^G(\Delta\chi) = \langle G_a|G_{a'}\rangle \sum_{|m| \leq N-1} e^{-im\Delta\chi} \left|S_{(N-1)m}^G\right|^2, \tag{32}$$

and appears to be simply proportional to the auto-correlation function of $G$. For $a = a'$, this result states that the auto-correlations of $G$ and $G_a$ are proportional. The control of directionality of $G$ through the auto-correlation function is therefore preserved through kernel dilation. For $a \neq a'$, this result essentially ensures that the kernel dilation does not introduce any unexpected distortion in the shape of the function in real space on $S^2$.

In addition to the auto-correlation function, symmetry properties may also be imposed on the spherical harmonic coefficients $\widehat{G}_{lm}$, which translate into simple directionality properties in real space for $G$. First, in the framework of a wavelet analysis on the sphere, one generally imposes the symmetry relation $\widehat{G}_{lm}^* = (-1)^m \widehat{G}_{l(-m)}$ in order to restrict to real analysis functions: $G(\theta, \varphi) \in \mathbb{R}$. Secondly, the constraint that $\widehat{G}_{lm}$ has non-zero values only for even or odd values $m \in T_N$, for any azimuthal band limit $N$, implies that the function $G$ is, respectively, even or odd under a rotation around itself by $\chi = \pi$: $G(\theta, \varphi + \pi) = (-1)^{N-1}G(\theta, \varphi)$. Thirdly, for such functions, the additional constraint that the spherical harmonic coefficients $\widehat{G}_{lm}$ are real for even values of $N - 1$, and purely imaginary for odd values of $N - 1$, implies that the function $G$ is, respectively, even or odd under a change in sign on $\varphi$: $G(\theta, -\varphi) = (-1)^{N-1}G(\theta, \varphi)$. These symmetries are defined up to a rotation of the function around itself by any angle $\chi \in [0, 2\pi)$, which amounts to a multiplication of the spherical harmonic coefficients $\widehat{G}_{lm}$ by a complex phase $e^{-im\chi}$. The three properties discussed are obviously preserved through kernel dilation of factorized functions. They indeed only concern the directionality coefficients $S_{lm}^G$, which are not affected by the kernel dilation.

In summary, the auto-correlation function and additional symmetries define directionality properties of a function. We have shown that the directionality properties studied are essentially preserved through kernel dilation of factorized steerable functions with compact harmonic support. Again, the verification of more precise directionality properties in real space for a function designed from its spherical harmonic coefficients unavoidably requires a numerical evaluation of sampled values of that function.

# 4 WAVELETS FROM KERNEL DILATION

In this section, we begin with the derivation of a new continuous wavelet formalism from the kernel dilation with continuous scales, and for factorized steerable wavelets with compact harmonic support. We then derive the scale-discretized wavelet formalism from the continuous wavelet formalism. The transition is performed through an integration of the dilation factor by slices. We emphasize

the practical accessibility of an exact reconstruction of band-limited signals from a finite number of analysis scales. We also illustrate these developments through the explicit design of an example scale-discretized wavelet. We finally recast the scale-discretized wavelet formalism developed in a generic invertible filter bank perspective.

## 4.1 Continuous wavelets

We simply consider the continuous wavelet formalism exposed in Section 2, and particularize it to the kernel dilation defined in Section 3. Hence, the scales of analysis are still continuous. The translations by $\omega_0 \in S^2$ and proper rotations by $\chi \in [0, 2\pi)$ of the wavelets are still defined through the continuous three-dimensional rotations from relations (2) and (3).

For application of the kernel dilation, we consider continuous factorized steerable functions $\Psi \in L^2(S^2, d\Omega)$ with compact harmonic support:

$$\widehat{\Psi}_{lm} = \tilde{K}_\Psi(l) S_{lm}^\Psi, \tag{33}$$

for a continuous kernel defined by a positive real function $\tilde{K}_\Psi(k) \in \mathbb{R}_+$ and a directional split defined by the directionality coefficients $S_{lm}^\Psi$. The compact harmonic support of the wavelet in the interval $l \in (\lfloor\alpha^{-1}B\rfloor, B)$ is ensured by a kernel $\tilde{K}_\Psi(k)$ with compact support in the interval $k \in (\alpha^{-1}B, B)$, with a compactness $c(\alpha) = \alpha/(\alpha - 1) \in [1, \infty)$:

$$\tilde{K}_\Psi(k) = 0 \quad \text{for} \quad k \notin (\alpha^{-1}B, B). \tag{34}$$

The steerability of a wavelet with an azimuthal band limit $N$ in ensured by the directional split:

$$S_{lm}^\Psi = 0 \quad \text{for all} \quad l, m \quad \text{with} \quad |m| \geq N, \tag{35}$$

with

$$\sum_{|m| \leq \min(N-1,l)} \left|S_{lm}^\Psi\right|^2 = 1, \tag{36}$$

for all $l \in \mathbb{N}^0$. Continuous axisymmetric wavelets $A(\theta)$ with compact harmonic support are simply obtained by the trivial directional split with $S_{lm}^A = \delta_{m0}$ for all $l \in \mathbb{N}^0$.

The analysis of a signal $F \in L^2(S^2, d\Omega)$ with the analysis function $\Psi$ gives the wavelet coefficients $W_\Psi^F(\rho, a)$ at each continuous scale $a$, around each point $\omega_0$, and in each orientation $\chi$, through the directional correlation (4). The reconstruction of $F$ from its wavelet coefficients results from relation (7). The zero mean condition (15) for the admissibility of $\Psi$ implies $\tilde{K}_\Psi^2(0) = 0$. One can also set arbitrarily $S_{00}^\Psi = 0$. The admissibility condition (16) summarizes to

$$0 < C_\Psi = \int_{(\alpha^{-1}B,B)} \frac{dk'}{k'} \tilde{K}_\Psi^2(k') < \infty, \tag{37}$$

which actually also encompasses the zero mean condition. The coefficients entering the reconstruction formula are $C_\Psi^l = 8\pi^2 C_\Psi/(2l + 1)$ for $l \in \mathbb{N}^0$. In other words, the kernel must formally be identified with the Fourier transform of an axisymmetric wavelet on the plane.

Note that for a factorized wavelet $\Psi$, the directional correlation defining the analysis of a signal may also be understood as a double correlation, by the kernel and the directional split successively. The standard correlation (9) of the signal $F$ and the axisymmetric wavelets defined by the kernel of $\Psi$, provides intermediate wavelet coefficients $W_{\tilde{K}_\Psi}^F(\omega_0, a)$ on $S^2$ at each scale $a \in \mathbb{R}_+^*$. The spherical harmonic transform of these coefficients reads as

$$\left(\widehat{W_{\tilde{K}_\Psi}^F}\right)_{lm}(a) = \sqrt{\frac{4\pi}{2l + 1}} \tilde{K}_\Psi(al) \widehat{F}_{lm}. \tag{38}$$

At each scale $a$, the directional correlation of the intermediate signal obtained at that scale $W^F_{\tilde{K}_\Psi}(\omega_0, a)$ and a directional wavelet defined by the directional split of $\Psi$ provides the final wavelet coefficients on SO(3):

$$\widehat{(W^F_\Psi)}^l_{mn}(a) = \frac{8\pi^2}{2l+1}\left(\sqrt{\frac{2l+1}{4\pi}}S^\Psi_{ln}\right)^* \widehat{(W^F_{\tilde{K}_\Psi})}_{lm}(a). \tag{39}$$

This reasoning obviously holds independently of the steerability or compact harmonic support properties of $\Psi$.

In conclusion, the definition of the kernel dilation provides a new continuous wavelet formalism, where scales, translations, and proper rotations of the wavelets are all continuous. As the previously developed continuous wavelet formalism based on the stereographic dilation, it finds application in the identification of local directional features of signals on the sphere. The wavelets defined bear new properties of compact harmonic support and steerability, which are preserved through kernel dilation. These properties can give a new insight for the analysis of local directional features. However, as already discussed the continuous scales required for the analysis prevent in practice the exact reconstruction of the signals analysed from their wavelet coefficients.

## 4.2 Scale-discretized wavelets

Scale-discretized wavelets $\Gamma$ can simply be obtained from continuous wavelets through an integration by slices of the dilation factor $a \in \mathbb{R}^*_+$. Through this transition procedure, scale-discretized wavelets remain factorized steerable functions with compact harmonic support, and are dilated through kernel dilation.

We consider the analysis of a signal $F \in L^2(S^2, d\Omega)$ with the band limit $B$. The original continuous wavelet $\Psi \in L^2(S^2, d\Omega)$ with a compact support is defined in the interval $k \in (\alpha^{-1}B, B)$. The value $\alpha > 1$ regulates the compactness $c(\alpha)$ of $\Psi$. It is also taken as a basis dilation factor. The discrete dilation factors for the scale-discretized wavelet will correspond to integer powers $\alpha^j$, for analysis depths $j \in \mathbb{N}$.

The scale-discretized wavelet $\Gamma \in L^2(S^2, d\Omega)$ is thus defined in factorized form:

$$\hat{\Gamma}_{lm} = \tilde{K}_\Gamma(l)\, S^\Gamma_{lm}, \tag{40}$$

for a scale-discretized kernel defined by a positive real function $\tilde{K}_\Gamma(k) \in \mathbb{R}_+$ and a directional split defined by the directionality coefficients $S^\Gamma_{lm}$. The directional split of $\Gamma$ is identified with the split of $\Psi$:

$$S^\Gamma_{lm} = S^\Psi_{lm}, \tag{41}$$

also giving

$$S^\Gamma_{lm} = 0 \quad \text{for all} \quad l, m \quad \text{with} \quad |m| \geq N, \tag{42}$$

and

$$\sum_{|m|\leq\min(N-1,l)} \left|S^\Gamma_{lm}\right|^2 = 1, \tag{43}$$

for $l \in \mathbb{N}^0$, while $S^\Gamma_{00} = 0$. The exact same steerability properties are therefore obviously shared by the continuous wavelet and the scale-discretized wavelet, independently of any dilation factor. The scale-discretized kernel $\tilde{K}_\Gamma(k)$ is obtained from the continuous kernel $\tilde{K}_\Psi(k)$ through an integration by slices of the dilation factor $a \in \mathbb{R}^*_+$ of the continuous wavelet formalism.

As a first step, a positive real *scaling function* $\tilde{\Phi}_\Gamma(k) \in \mathbb{R}_+$ of a continuous variable $k \in \mathbb{R}_+$, is defined which gathers the largest

dilation factors $a \in (1, \infty)$, or correspondingly the lowest values of $k$. This generating function reads for $k \in \mathbb{R}^*_+$ as

$$\tilde{\Phi}^2_\Gamma(k) = \frac{1}{C_\Psi} \int_1^\infty \frac{da}{a}\, \tilde{K}^2_\Psi(ak)$$
$$= \frac{1}{C_\Psi} \int_{(\alpha^{-1}B, B) \cap (k, \infty)} \frac{dk'}{k'}\, \tilde{K}^2_\Psi(k'), \tag{44}$$

and continuously continuated at $k = 0$ by $\tilde{\Phi}^2_\Gamma(k) = 1$. The scaling function $\tilde{\Phi}^2_\Gamma(k)$ therefore decreases continuously from unity down to zero in the interval $k \in (\alpha^{-1}B, B)$:

$$\tilde{\Phi}^2_\Gamma(k) = 1 \quad \text{for} \quad 0 \leq k \leq \alpha^{-1}B,$$
$$\tilde{\Phi}^2_\Gamma(k) \in (0, 1) \quad \text{for} \quad \alpha^{-1}B < k < B,$$
$$\tilde{\Phi}^2_\Gamma(k) = 0 \quad \text{for} \quad k \geq B. \tag{45}$$

Note that similar procedures of scale integration by slices were already proposed in the development of corresponding formalisms on the plane (Duval-Destin et al. 1993; Muschietti & Torrésani 1995; Vandergheynst & Gobbers 2002).

As a second step, a simple Littlewood–Paley decomposition (Frazier et al. 1991) is used to define the scale-discretized kernel $\tilde{K}_\Gamma(k)$ by subtracting the scaling function $\tilde{\Phi}_\Gamma(k)$ to its contracted version $\tilde{\Phi}_\Gamma(\alpha^{-1}k)$. This implicitly sets the value $\alpha$ as the basis dilation factor. The scale-discretized kernel also reads as an integration of the continuous kernel over a slice $a \in (\alpha^{-1}, 1)$ for the dilation factor, or equivalently over a slice $k \in (\alpha^{-1}B, B)\cap(\alpha^{-1}k, k)$ of the compact support interval:

$$\tilde{K}^2_\Gamma(k) = \tilde{\Phi}^2_\Gamma(\alpha^{-1}k) - \tilde{\Phi}^2_\Gamma(k)$$
$$= \frac{1}{C_\Psi} \int_{\alpha^{-1}}^1 \frac{da}{a}\, \tilde{K}^2_\Psi(ak)$$
$$= \frac{1}{C_\Psi} \int_{(\alpha^{-1}B, B)\cap(\alpha^{-1}k, k)} \frac{dk'}{k'}\, \tilde{K}^2_\Psi(k'). \tag{46}$$

The scale-discretized kernel therefore has a compact support in the interval $k \in (\alpha^{-1}B, \alpha B)$:

$$\tilde{K}_\Gamma(k) = 0 \quad \text{for} \quad k \notin (\alpha^{-1}B, \alpha B). \tag{47}$$

This support is wider than for the original continuous kernel and the scaling function. The corresponding compactness reads as $c(\alpha^2) = \alpha^2/(\alpha^2 - 1) \in [1, \infty)$. The compact harmonic support of the scale-discretized wavelet $\Gamma$ itself is thus defined in the interval $l \in (\lfloor\alpha^{-1}B\rfloor, \lceil\alpha B\rceil)$. The kernel also satisfies $\tilde{K}^2_\Gamma(0) = 0$, leading to a scale-discretized wavelet $\Gamma$ with a zero mean on the sphere:

$$\frac{1}{4\pi} \int_{S^2} d\Omega\, \Gamma(\omega) = 0. \tag{48}$$

The dilations by $\alpha^j$ of the scale-discretized wavelet obtained are defined by the kernels $\tilde{K}_\Gamma(\alpha^j k)$ for any analysis depth $j \in \mathbb{N}$. Each kernel has a compact support in the interval $k \in (\alpha^{-(1+j)}B, \alpha^{(1-j)}B)$ and exhibits a maximum in $k = \alpha^{-j}B$, with $\tilde{K}_{\Gamma_{\alpha^j}}(\alpha^{-j}B) = 1$. The scale-discretized wavelet $\Gamma_{\alpha^j}$ at each analysis depth $j$ thus has a compact harmonic support in the interval $l \in (\lfloor\alpha^{-(1+j)}B\rfloor, \lceil\alpha^{(1-j)}B\rceil)$. The property $\tilde{K}^2_\Gamma(0) = 0$ still ensures that each scale-discretized wavelet has a zero mean on the sphere. Note that for $j \geq 1$, one gets a dilation factor strictly greater than unity $\alpha^j > 1$, and the scale-discretized wavelet has a band limit lower or equal to the assumed band limit $B$ for the signal $F$ to be analysed. At $j = 0$, only the values of the kernel in the interval $l \in (\lfloor\alpha^{-1}B\rfloor, B)$ are of interest, as higher frequencies $l$ are truncated by the signal $F$ itself through the directional correlation. One can equivalently consider that the compact support of the kernel is restricted to $k \in (\alpha^{-1}B, B)$

in the definition of the scale-discretized wavelet at this first analysis depth $j = 0$. For $j \leq -1$, the lower bound of the compact harmonic support of the scale-discretized wavelet is larger than the band limit $B$. The scale-discretized wavelets with negative analysis depths can therefore be discarded, as the result of their directional correlation with the signal $F$ would be identically zero.

The admissibility condition (37) for continuous wavelets simply turns into a resolution of the identity below the band limit by a set of dilated wavelets at various analysis depths $j$, with $0 \leq j \leq J$, and a dilated scaling function at some total analysis depth $J \in \mathbb{N}$. One gets, in particular, for $0 \leq k = l < B$:

$$\tilde{\Phi}_\Gamma^2\left(\alpha^J l\right) + \sum_{j=0}^{J} \tilde{K}_\Gamma^2(\alpha^j l) = 1. \tag{49}$$

The scaling function values $\tilde{\Phi}_\Gamma(\alpha^J l)$ are equal to unity in the interval $l \in [0, \lfloor \alpha^{-(1+J)} B \rfloor]$, then decrease in the interval $l \in (\lfloor \alpha^{-(1+J)} B \rfloor, \lceil \alpha^{-J} B \rceil)$, and are equal to zero for $l \geq \lceil \alpha^{-J} B \rceil$. The kernel values $\tilde{K}_\Gamma(\alpha^j l)$ are non-zero only in the compact harmonic support interval $l \in (\lfloor \alpha^{-(1+j)} B \rfloor, \lceil \alpha^{(1-j)} B \rceil)$. The scaling function typically retains the low frequency part of the signal, which will not be analysed. All signal information at frequencies $l \leq \lfloor \alpha^{-(1+J)} B \rfloor$ is kept only in the scaling function, equal to unity. The wavelets are equal to zero at these frequencies. All signal information at frequencies $l \geq \lceil \alpha^{-J} B \rceil$ is fully analysed by the wavelets, while the scaling function is equal to zero. Intermediate frequencies are also analysed by the wavelets but the scaling function is required for the reconstruction of the corresponding signal information.

Let us define the maximum analysis depth $J_B(\alpha)$ as the lowest integer value such that $\alpha^{-J_B(\alpha)} B \leq 1$:

$$J_B(\alpha) = \lceil \log_\alpha B \rceil. \tag{50}$$

In a case where the total analysis depth would be chosen strictly above $J_B(\alpha)$, all wavelets at analysis depths $j$ with $J \geq j \geq J_B(\alpha) + 1$ would be identically null as their kernel have a compact support strictly included in the interval $k \in (0, 1)$. The total analysis depth is consequently naturally limited by $J \leq J_B(\alpha)$. In the case $J = J_B(\alpha)$, the dilated scaling function evaluated at $\alpha^{J_B(\alpha)} l$ has a non-zero value only at $l = 0$, $\tilde{\Phi}_\Gamma^2(\alpha^{J_B(\alpha)} l) = \delta_{l0}$, while all wavelets are equal to zero at $l = 0$ as they have a zero mean. Hence, the identity can be resolved with $J_B(\alpha) + 1$ dilated wavelets and a trivial scaling function which simply retains the spherical harmonic coefficient $\hat{F}_{00}$ out of the analysis, or equivalently the mean of the signal over the sphere. One gets, in particular, for $0 \leq k = l < B$:

$$\delta_{l0} + \sum_{j=0}^{J_B(\alpha)} \tilde{K}_\Gamma^2(\alpha^j l) = 1. \tag{51}$$

## 4.3 Analysis and exact reconstruction

Following the scale discretization defining the wavelets $\Gamma \in L^2(S^2, d\Omega)$, a new scale-discretized wavelet formalism is provided for the analysis and the exact reconstruction of band-limited signals.

The analysis of a band-limited signal $F \in L^2(S^2, d\Omega)$ with the band limit $B$, with a scale-discretized wavelet $\Gamma$ is performed by directional correlations just as in the continuous wavelet formalism. The translations by $\omega_0 \in S^2$ and proper rotations by $\chi \in [0, 2\pi)$ of the wavelets are still defined through the continuous three-dimensional rotations from relations (2) and (3). At each analysis depth $j$ with $0 \leq j \leq J \leq J_B(\alpha)$, the analysis is performed by directional correlations of $F$ with the analysis functions $\Gamma_{\alpha^j}$ dilated through the kernel

dilation by dilation factors $\alpha^j$:

$$W_\Gamma^F(\rho, \alpha^j) = \langle \Gamma_{\rho, \alpha^j} | F \rangle. \tag{52}$$

At each discrete scale $\alpha^j$, the wavelet coefficients $W_\Gamma^F(\rho, \alpha^j)$ still identify a square-integrable function on SO(3), and characterize the signal around each point $\omega_0$, and in each orientation $\chi$. Once more, the direct Wigner $D$-function transform of the wavelet coefficients is given as the point-wise product of the spherical harmonic coefficients of the signal and the wavelet:

$$\widehat{\left(W_\Gamma^F\right)}_{mn}^l(\alpha^j) = \frac{8\pi^2}{2l+1} \widehat{(\Gamma_{\alpha^j})}_{ln}^* \hat{F}_{lm}. \tag{53}$$

Again, the factorization relation (40) allows one to understand the directional correlation (53) as a double correlation, by the kernel and the directional split successively.

The reconstruction of the band-limited signal $F$ from its wavelet coefficients reads in terms of a summation on a finite number $J + 1$ of discrete dilation factors:

$$F(\omega) = [\Phi_{\alpha^J} F](\omega)$$
$$+ \sum_{j=0}^{J} \int_{SO(3)} d\rho \, W_\Gamma^F(\rho, \alpha^j) \left[ R(\rho) L^d \Gamma_{\alpha^j} \right](\omega). \tag{54}$$

The approximation $[\Phi_{\alpha^J} F](\omega)$ accounts for the part of the signal retained in the scaling function $\tilde{\Phi}_\Gamma(\alpha^J l)$. In a very similar way to the part of the signal analysed by the wavelets, it can be written as

$$[\Phi_{\alpha^J} F](\omega) = 2\pi \int_{S^2} d\Omega_0 \, W_\Phi^F\left(\omega_0, \alpha^J\right) \left[ R(\omega_0) L^d \Phi_{\alpha^J} \right](\omega), \tag{55}$$

with $W_\Phi^F(\omega_0, \alpha^J) = \langle \Phi_{\omega_0, \alpha^J} | F \rangle$, and for an axisymmetric function $\Phi \in L^2(S^2, d\Omega)$ defined by $\widehat{(\Phi_\Gamma)}_{lm} = \tilde{\Phi}_\Gamma(l) \delta_{m0}$. In the particular case where $J = J_B(\alpha)$, one gets $\widehat{(\Phi_\Gamma)}_{lm} = \delta_{l0} \delta_{m0}$ and the approximation simply reduces to the mean of the signal over the sphere: $[\Phi_{\alpha^{J_B(\alpha)}} F] = (4\pi)^{-1} \int_{S^2} d\Omega \, F(\omega)$. The zero mean signal is completely analysed by the scale-discretized wavelets. The operator $L^d$ in $L^2(S^2, d\Omega)$ in the present scale-discretized wavelet formalism is defined by the following action on the spherical harmonic coefficients of functions: $\widehat{L^d G}_{lm} = (2l + 1)\hat{G}_{lm}/8\pi^2$. This operator defining the scale-discretized wavelets $L^d \Gamma_{\alpha^j}$ used for reconstruction is independent of $\Gamma$, contrarily to the operator $L_\Psi$ for continuous wavelets. This simply comes from the fact that the scale-discretized wavelets are, through their definition (46), normalized by $C_\Psi$.

Just as in the continuous wavelet formalism where the admissibility condition (37) is required, the present reconstruction formula holds if and only if the scale-discretized wavelet satisfies the constraints (43), and (49) or (51). These constraints are automatically satisfied by construction of the scale-discretized wavelets through the integration by slices. Again, this corresponds to the requirement that the wavelet family as a whole, including the scaling function, preserves the signal information at each frequency $l \in \mathbb{N}$.

Let us emphasize the fact that a finite number of discrete dilation factors is required for the analysis and reconstruction of a band-limited signal. Contrarily to the case of the continuous dilation factors, this allows exact reconstruction of band-limited signals from relation (54). The translations and proper rotations of the wavelets are still defined through the continuous three-dimensional rotations. As discussed in Section 2.1, the exact reconstruction is achieved only for suitable pixelizations of $\rho = (\varphi_0, \theta_0, \chi)$ which provide an exact quadrature rule for the numerical integration of band-limited functions on SO(3). In the case of non band-limited signals, an infinite number of negative analysis depths $j \leq -1$ should be added for a complete analysis. This would break the possibility of

exact reconstruction. However, in any case, no exact quadrature rule exists on SO(3) for the numerical integration of non band-limited functions, which already prevents an exact numerical analysis.

Let us also remark that scale-discretized axisymmetric wavelets with compact harmonic support and dilated through kernel dilation were recently introduced under the name of needlets (Baldi et al. 2006; Guilloux et al. 2007; Marinucci et al. 2007). It is possible to show that the needlet coefficients of a wide class of random signals on the sphere are uncorrelated in the asymptotic limit of small scales, at any fixed angular distance on $S^2$. The scale-discretized steerable wavelets with compact harmonic support, thanks to their factorized form and to the choice of the kernel dilation, are also good candidates for a directional extension of needlets.

### 4.4 Example wavelet design

As an illustration of the transition between the continuous and scale-discretized formalisms, we explicitly design a real scale-discretized factorized steerable wavelet $\Gamma$ with compact harmonic support, from a real continuous wavelet $\Psi$. We first define the directional split and kernel with generic values for the band limit $B$, for the basis dilation factor $\alpha > 1$, as well as for the azimuthal band limit $N$ of steerability. We then illustrate the definition for particular values. The directionality coefficients of $\Psi$ and $\Gamma$ are identical by the definition (41). The steerability relation (42) is imposed with an azimuthal band limit $N$. The function is imposed to be real and to be even or odd both under rotation around itself by $\pi$ and under a change of sign on $\varphi$. As discussed in Section 3.1, this corresponds to the constraints that only the $T = N$ values $m \in T_N$ are allowed, with $S_{lm}^{\Gamma*} = (-1)^m S_{l(-m)}^{\Gamma}$, and $S_{lm}^{\Gamma}$ is real for even values of $N - 1$, and purely imaginary for odd values of $N - 1$. One has $S_{00}^{\Gamma} = 0$, and only the values $S_{lm}^{\Gamma}$ with $1 \leq l < B$ and $0 \leq m \leq l$ and $m \in T_N$ need to be defined explicitly. These values are set in order to ensure a precise structure of the auto-correlation function (29) under the constraint (43):

$$S_{lm}^{\Gamma} = \eta_N \beta_{(N,m)} \left[ \frac{1}{2^{\gamma_{(N,l)}}} \left( \frac{\gamma_{(N,l)}}{\frac{\gamma_{(N,l)} - m}{2}} \right) \right]^{1/2}, \tag{56}$$

with $\eta_N = 1$ for even values of $N - 1$, $\eta_N = i$ for odd values of $N - 1$, $\beta_{(N,m)} = [1 - (-1)^{N+m}]/2$, and $\gamma_{(N,l)} = \min(N - 1, l - [1 + (-1)^{N+l}]/2)$. The auto-correlation function follows as

$$C^{\Gamma}(\Delta\chi) = \sum_{l \in (\lfloor \alpha^{-1}B \rfloor, B)} \tilde{K}_{\Gamma}^2(l) \cos^{\gamma_{(N,l)}}(\Delta\chi). \tag{57}$$

When $N - 1 > \lfloor \alpha^{-1}B \rfloor + 1$, the peakedness of the auto-correlation is generically defined by the powers $\gamma_{(N,l)}$ of $\cos(\Delta\chi)$ at each value of $l$. This expresses the simple fact that the azimuthal frequency index $m$ must always remain bounded in absolute value by the overall frequency index: $|m| \leq l$. However, the values $\gamma_{(N,l)}$ ensure that the directionality coefficients are independent of $l$ for $l \geq N - 1$. Hence, when $N - 1 \leq \lfloor \alpha^{-1}B \rfloor + 1$, the auto-correlation function takes the form

$$C^{\Gamma}(\Delta\chi) = ||\Gamma||^2 \cos^{(N-1)}(\Delta\chi), \tag{58}$$

with $||\Gamma||^2 = \sum_{l \in (\lfloor \alpha^{-1}B \rfloor, B)} \tilde{K}_{\Gamma}^2(l)$. Its peakedness increases as the power $N - 1$ of $\cos(\Delta\chi)$. The cost for the corresponding increase in directionality with $N$ is of course that a larger number of basis functions is required to steer the wavelet.

Let us emphasize the importance of the structure (57) in the global scheme of the scale-discretized wavelet formalism. The azimuthal band limit $N$ might be considered much smaller than the lower bound of the compact harmonic support interval for the first analysis depth $j = 0$: $N \ll \lfloor \alpha^{-1}B \rfloor$. However at each analysis depth $j \geq 1$, the compact harmonic support is defined in the interval $l \in (\lfloor \alpha^{-(1+j)}B \rfloor, \lceil \alpha^{(1-j)}B \rceil)$. Hence, the structure (58) of the auto-correlation function breaks down to (57) at a given analysis depth $j_N$, defined as the lowest integer such that $N - 1 > \lfloor \alpha^{-(1+j_N)}B \rfloor + 1$. If one wants to preserve the structure (58) for all dilated wavelets, the resolution of the identity (49) can be used up to a total analysis depth $J = j_N - 1$.

The continuous kernel is defined from a Schwartz function with compact support in the interval $(-1, 1)$ on $\mathbb{R}$ as

$$\tilde{K}_\Psi(k) = \exp\left[ -\frac{1}{1 - t^2(k)} \right] \quad \text{for} \quad t(k) \in (-1, 1),$$
$$\tilde{K}_\Psi(k) = 0 \quad \text{for} \quad t(k) \notin (-1, 1), \tag{59}$$

for the function

$$t(k) = 2\frac{\alpha k - B}{(\alpha - 1)B} - 1, \tag{60}$$

which linearly maps the compact support interval $k \in (\alpha^{-1}B, B)$ on to $t \in (-1, 1)$. The function $\tilde{K}_\Psi(k)$ is infinitely differentiable for $k \in \mathbb{R}_+$. It notably exhibits a maximum at the centre $t(k) = 0$ of the support interval and smoothly drops down to zero at the interval bounds. Let us recall that the kernel (59) is by definition taken as a positive function. An overall change of sign would simply flip the sign of the wavelet at each point in real space. The scaling function $\tilde{\Phi}_\Gamma(k)$ and scale-discretized kernel $\tilde{K}_\Gamma(k)$ follow from relations (44) and (46), respectively. The scaling function for values in the interval $k \in (\alpha^{-(1+j)}B, \alpha^{-j}B)$ for each analysis depth $j$ can be obtained by numerical integration. Note that the exactness of reconstruction provided by the formalism is not affected by such a numerical integration, as long as the scale-discretized kernels are simply defined by differences of scaling functions through relation (46). Corresponding graphs are reported in Fig. 1 for a band limit $B = 1024$ and a basis dilation factor $\alpha = 2$ associated with a standard dyadic decomposition of scales.

Plots of the scale-discretized wavelet are reported at various analysis depths in Fig. 2, for $B = 1024$, $\alpha = 2$, and for an azimuthal band limit $N = 3$ for the steerability. These plots notably illustrate localization and directionality properties of the wavelet.

### 4.5 Invertible filter bank

A scale-discretized wavelet formalism with relations (49) and (51) for factorized steerable wavelets with compact harmonic support can be developed by simply relying on a Littlewood–Paley decomposition, without any contact with the continuous wavelet formalism. One simply needs to choose any arbitrary scaling function satisfying relation (45) and define the corresponding scale-discretized kernels by differences of scaling functions at successive scales.

Such invertible filter banks based on the harmonic dilation were already developed in the case of axisymmetric wavelets (Starck et al. 2006b), and our definition of factorized steerable wavelets with compact harmonic support allows a straightforward generalization to directional wavelets with the kernel dilation. Also notice that the constraints of steerability and compact harmonic support for the scale-discretized wavelets can technically be relaxed without affecting the Littlewood–Paley decomposition. However both properties are essential for the control of localization and directionality properties through kernel dilation. Moreover, in the absence of compact harmonic support, the relation (49) turns into a resolution of the contracted scaling function $\tilde{\Phi}_\Gamma^2(\alpha^{-1}l)$ which differs from unity below the band limit. In other words, the filter bank developed in
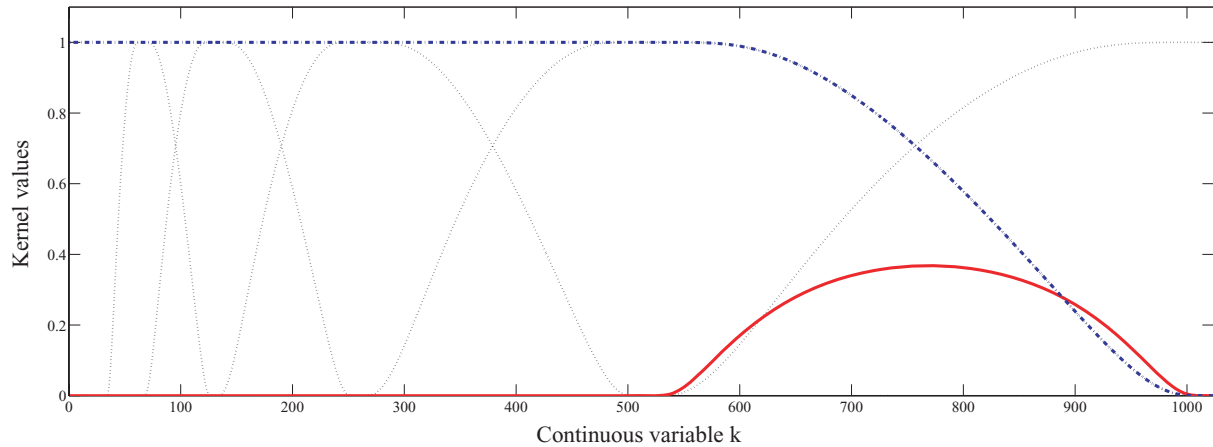
**Figure 1.** Graphs of the continuous kernel defined in (59) and (60), and the corresponding scale-discretized kernels obtained by differences of scaling functions at various analysis depths. A band limit $B = 1024$ and a basis dilation factor $\alpha = 2$ are chosen. The continuous kernel $\tilde{K}_\Psi(k)$ is represented by the continuous red line. The numerically integrated scaling function $\tilde{\Phi}_\Gamma(k)$ is represented by the dot–dashed blue line. The scale-discretized kernels $\tilde{K}_\Psi(2^j k)$ are plotted as the dotted black lines for the five first analysis depths $j$, with $0 \leq j \leq 4$. For $j = 0$, the corresponding compact support interval is cut at the band limit: $k \in (512, 1024)$. For $1 \leq j \leq 4$ as for all larger analysis depths (not shown), the intervals progressively move to lower frequencies and shrink: $k \in (256/2^{(j-1)}, 1024/2^{(j-1)})$. At the maximum analysis depth $j = J_B(\alpha) = 10$, the compact support is shrunk to $k \in (0.5, 2)$ and the scale-discretized kernel only contains the frequency $l = 1$.
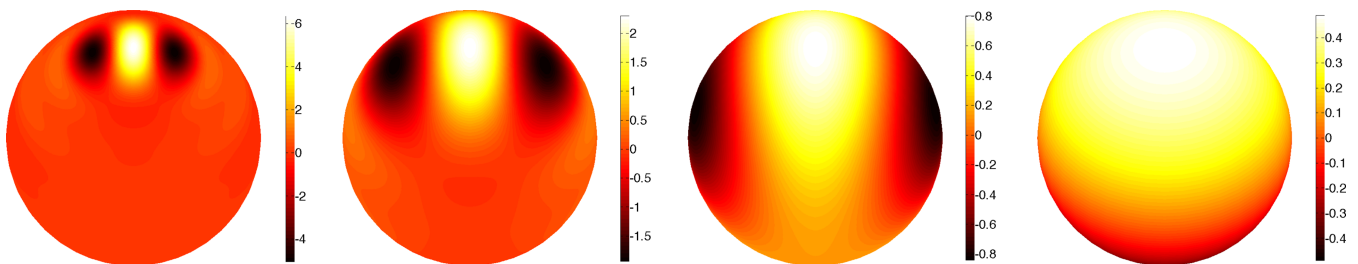


**Figure 2.** Plots of the real scale-discretized wavelets defined through relations (56), (59) and (60), at various analysis depths. A global band limit $B = 1024$ and a basis dilation factor $\alpha = 2$ are chosen, as well as an azimuthal band limit $N = 3$ for the steerability. The light and dark regions, respectively, correspond to positive and negative values of the functions (see value bars). The wavelets are neither translated, that is, they have their central position at the North Pole, nor rotated, {that is,} they are in their original orientation $\chi = 0$ (the meridian $\varphi = 0$ corresponds to a vertical line passing by the North Pole). The wavelets are represented at the four largest analysis depths, $7 \leq j \leq 10 = J_B(\alpha)$, identifying the four largest scales. At $j = 7$ (extreme left-hand panel), $j = 8$ (centre left-hand panel), and $j = 9$ (centre right-hand panel), the compact supports of the scale-discretized kernels, respectively, contain the frequencies $l = 5$ to 15 with a kernel maximum at $l = 8$, $l = 3$ to 7 with a kernel maximum at $l = 4$, and $l = 2$ to 3 with a kernel maximum at $l = 2$. At $j = 10$ (extreme right-hand panel), the scale-discretized kernel only contains the frequency $l = 1$. In real space, the dispersion of angular distances around the central position on the sphere increases with the analysis depth, in complete coherence with the constraint (28). For the depths $j$ with $7 \leq j \leq 9$, the lowest frequencies $l$ are greater or equal to $N - 1 = 2$ and the azimuthal frequency indices contained in the directional split are $m \in \{-2, 0, 2\}$. These wavelets all have the same directionality property as measured by an auto-correlation function evolving as $\cos^2(\Delta\chi)$. For the depth $j = 10$, the scale-discretized wavelet is a pure dipole ($l = 1$). The azimuthal frequency index is restricted to $m = 0$, and the wavelet is simply axisymmetric with a constant auto-correlation function.

such a case analyses the part of the signal corresponding to its standard correlation with the contracted scaling function, rather than the signal itself. In the absence of compact harmonic support and steerability, essential multi-resolution properties are also lost (see Section 5.1). The memory and computation time requirements of the algorithm for the analysis and reconstruction of signals therefore increase significantly and may rapidly become overwhelming.

Invertible filter banks based on the stereographic dilation have also recently been proposed (Yeo et al. 2006), but they do not share these essential multi-resolution properties.

## 5 EXACT MULTI-RESOLUTION ALGORITHM

In this section, we identify the multi-resolution properties of the scale-discretized wavelet formalism developed. We describe a corresponding algorithm for the analysis and exact reconstruction of band-limited signals. We discuss in detail the memory and computation time requirements of the algorithm. Finally, an implementation of the algorithm is tested.

### 5.1 Multi-resolution

We consider the analysis and exact reconstruction of a band-limited signal $F \in L^2(S^2, d\Omega)$ with a scale-discretized wavelet $\Gamma \in L^2(S^2, d\Omega)$, which is a factorized steerable function with compact harmonic support. We consider a band limit $B$ and a basis dilation factor $\alpha > 1$.

The signal is identified by $\mathcal{O}(B^2)$ spherical harmonic coefficients $\widehat{F}_{lm}$. Equivalently, sampled values $F(\omega_i)$ of the signal on a number $\mathcal{O}(B^2)$ of points $\omega_i$ are generally required in order to describe it completely. The integer $i$ simply indexes the points of the chosen pixelization. Notably exact quadrature rules for integration of

band-limited signals on S$^2$ with the band limit $B$ exist on equiangular and Gauss–Legendre pixelizations on $\mathcal{O}(B^2)$ points. The quadrature rules on HEALPIX pixelizations on $\mathcal{O}(B^2)$ points are non-exact but can be made very precise (Driscoll & Healy 1994; Doroshkevich et al. 2005a; Górski et al. 2005).

The compact harmonic support of the scale-discretized wavelet $\Gamma_{\alpha^j}$ is reduced in the intervals $l \in (\lfloor \alpha^{-(1+j)}B \rfloor, \lceil \alpha^{(1-j)}B \rceil)$ through the kernel dilation at each analysis depth $j$. As a function on SO(3), the wavelet coefficients at depth $j$ exhibit the same compact harmonic support as the scale-discretized wavelet $\Gamma_{\alpha^j}$. From relation (53), the Wigner $D$-transform $(\widehat{W_\Gamma^F})_{mn}(\alpha^j)$ of the wavelet coefficients is indeed non-zero only in the same interval as the wavelet. In particular, the band limit of the wavelet coefficients is decreased to $\lceil \alpha^{(1-j)}B \rceil$ at depth $j$. Consequently, the number of sampled values of the wavelet coefficients is reduced at each increase in the analysis depths $j$ to $\alpha^{2(1-j)} \times \mathcal{O}(B^2)$ discrete points of the form $(\omega_0)_{i(j)}$ on S$^2$, where $i(j)$ simply indexes these points. The number of operations required for their computation is reduced correspondingly. Hence, the kernel dilation applied to scale-discretized wavelets with compact harmonic support provides a first strong multi-resolution property for the formalism.

The steerability of the wavelet is also important in the algorithmic structure of the analysis (Wiaux et al. 2005, 2006, 2007), beyond the fact that it ensures that directionality properties are preserved through kernel dilation. Indeed, by linearity of the directional correlation (52), the general property of steerability (23) is transferred from the wavelet to the wavelet coefficients of any signal. At each point $(\omega_0)_{i(j)}$ and at each analysis depth $j$, the wavelet coefficients of a signal $F$ with the scale-discretized wavelet $\Gamma_{\alpha^j}$ are known for all continuous rotation angles $\chi \in [0, 2\pi)$ as a linear combination of the wavelet coefficients of $F$ with $M$ basis wavelets. As discussed, the basis wavelets can be taken as specific rotations $\Gamma_{\chi_p, \alpha^j}$ of the wavelet on itself by rotation angles $\chi_p \in [0, 2\pi)$, with interpolation weights given as simple translations by $\chi_p$ of a unique function $k(\chi)$. We consider wavelets for which the number of rotations required can by optimized to $M = T \leq 2N - 1$, where $T$ is the finite number of values of $m$ for which $\widehat{G}_{lm}$ has a non-zero value for at least one value of $l$. Consequently, the steerability of the scale-discretized wavelet $\Gamma_{\alpha^j}$ implies a reduction of the number of sampled values of the wavelet coefficients to the $T$ values $\chi_p$ of the rotation angle, with $0 \leq p \leq T - 1$, at each point $(\omega_0)_{i(j)}$ and at each analysis depth $j$. The number of operations required for their computation is reduced correspondingly. From this perspective, steerability provides a second strong multi-resolution property for the formalism. All required sampled values of the wavelet coefficients of a signal with a steerable wavelet may be mapped on a sphere for each of the $T$ values of $\chi_p$, at each analysis depth $j$.

In summary, when multi-resolution properties of the formalism are fully accounted for, a reduced number of discrete points of the form $\rho_{I(j)} = ((\omega_0)_{i(j)}, \chi_p)$ on SO(3) are required for the sampled values $W^F{}_\Gamma(\rho_{I(j)}, \alpha^j)$ of the wavelet coefficients, where $I(j) = \{i(j), p\}$ simply indexes these points at each analysis depth $j$.

## 5.2 Algorithm

The proposed algorithm works in harmonic space on S$^2$ and SO(3) in order to take advantage of the directional correlation relation (53).

Some pre-calculations are first required. The spherical harmonic coefficients $(\widehat{\Gamma_{\alpha^j}})_{lm}$ of the scale-discretized wavelets must be designed at each analysis depth $j$. A numerical integration can be

required in order to compute the scaling functions $\tilde{\Phi}_\Gamma^2(\alpha^j k)$ at all analysis depths from the spherical harmonic coefficients $\widehat{\Psi}_{lm}$ of a continuous wavelet in relation (44). The scale-discretized kernels $\tilde{K}_\Gamma^2(\alpha^j k)$ are then obtained by differences of scaling functions, and multiplied by the directional split chosen $S_{lm}^\Gamma$.

The analysis proceeds as follows. The band-limited signal $F$ is given in terms of its sampled values $F(\omega_i)$ on the $\mathcal{O}(B^2)$ discrete points $\omega_i$ of S$^2$. The spherical harmonic coefficients $\widehat{F}_{lm}$ of the signal are computed by quadrature through a direct spherical harmonic transform. The direct Wigner $D$-function transform $(\widehat{W_\Gamma^F})_{mn}(\alpha^j)$ of the wavelet coefficients is then simply obtained by the point-wise product (53). The computation of sampled values $W_\Gamma^F(\rho_{I(j)}, \alpha^j)$ of the wavelet coefficients requires an inverse Wigner $D$-function transform at each analysis depth $j$. Before reconstruction, any suitable analysis scheme can be applied on the wavelet coefficients, for typical purposes of denoising or deconvolution. This provides altered coefficients $\bar{W}_\Gamma^F(\rho_{I(j)}, \alpha^j)$. The reconstruction proceeds through the exact same operations as the analysis, in reverse order. The Wigner $D$-function coefficients $(\widehat{\bar{W}_\Gamma^F})_{mn}(\alpha^j)$ of the altered wavelet coefficients are computed by quadrature through a direct Wigner $D$-function transform at each analysis depth $j$. The spherical harmonic coefficients of the reconstructed signal $\widehat{\bar{F}}_{lm}$ are then obtained as a finite summation following from relations (54) and (55):

$$\widehat{\bar{F}}_{lm} = [\widehat{\Phi_{\alpha^J} F}]_{lm} + \frac{2l+1}{8\pi^2} \sum_{j=0}^{J} \sum_{|n| \leq \min(N-1,l)} (\widehat{\Gamma_{\alpha^j}})_{ln} (\widehat{\bar{W}_\Gamma^F})_{mn}^l (\alpha^j), \quad (61)$$

with

$$[\widehat{\Phi_{\alpha^J} F}]_{lm} = \tilde{\Phi}_\Gamma^2(\alpha^J l)\widehat{F}_{lm}. \quad (62)$$

In the particular case where $J = J_B(\alpha)$, one gets trivially $[\widehat{\Phi_{\alpha^J} F}]_{lm} = \delta_{l0}\delta_{m0}\widehat{F}_{00}$, which corresponds to keep only the mean of the signal out of the analysis.

The samples $\bar{F}(\omega_i)$ of the reconstructed signal are recovered by simple inverse spherical harmonic transform. If no alteration was applied to the wavelet coefficients, the exact same samples are obtained as for the original signal $F$. This exactness also obviously relies on the use of exact quadrature rules both for the direct spherical harmonic transform of the signal in the analysis part, and for the direct Wigner $D$-function transform of the wavelet coefficients in the reconstruction part. This requires the choice of equiangular or Gauss–Legendre pixelizations on S$^2$ defining the discrete points $\omega_i$ for the sampling of the original signal, and defining the discrete points $(\omega_0)_{i(j)}$ for the sampling the wavelet coefficients at each analysis depth $j$ and for each value $\chi_p$. Again HEALPIX pixelizations provide non-exact but very precise quadrature rules.

## 5.3 Memory requirements

We define the *storage redundancy* of the algorithm as the ratio of the number of sampled values of the wavelet coefficients at all analysis depths with a scale-discretized wavelet, to the number of sampled values of the original signal itself. A low storage redundancy is important for achieving as low memory requirements as possible in a practical implementation of the algorithm.

The Wigner $D$-transform $(\widehat{W_\Gamma^F})_{mn}(\alpha^j)$ of the wavelet coefficients is non-zero only in the interval $l \in (\lfloor \alpha^{-(1+j)}B \rfloor, \lceil \alpha^{(1-j)}B \rceil)$ at each analysis depth $j$. Each frequency index $l$ is thus retained exactly twice when all analysis depths $j$ are considered. Moreover, for a

steerable wavelet with azimuthal band limit $N$, the index $n$ accounting for the wavelet directionality in relations (53) and (61) takes by definition $T$ values, with $T \leq 2N - 1$. On the contrary, the index $m$ is only related to the signal. Consequently, the storage redundancy of the algorithm would be exactly $2T$ if the wavelet coefficients were to be computed in harmonic space only.

However, the computation of the sampled values $W_\Gamma^F(\rho_{I(j)}, \alpha^j)$ of the wavelet coefficients in real space on the discrete points $\rho_{I(j)} = ((\omega_0)_{i(j)}, \chi_p)$ of SO(3) is of course essential for general analysis purposes. Let us recall that a number $\alpha^{2(1-j)} \times \mathcal{O}(B^2)$ of discrete points $(\omega_0)_{i(j)}$ on S$^2$ is required at each analysis depth $j$. This number of sampled values is restricted by the band limit but not by the existence of a lower bound of the compact harmonic support. Thanks to the steerability, only $M = T$ values $\chi_p$ are required at each point $(\omega_0)_{i(j)}$. The storage redundancy of the algorithm is thus obtained by accounting for the steerability and summing over all analysis depths $j$ with $0 \leq j \leq J$. In the most exacting case where $J = J_B(\alpha)$, it simply reads as

$$[R_\mathrm{s}]_{(B,T)}(\alpha) = \left[1 + c(\alpha^2)\left(1 - \alpha^{-2J_B(\alpha)}\right)\right] T. \tag{63}$$

Let us recall that $c(\alpha^2) = \alpha^2/(\alpha^2 - 1) \in [1, \infty)$ stands for the compactness of the scale-discretized wavelet. The number of the sampled values $W_\Gamma^F(\rho_{I(j)}, \alpha^j)$ of the wavelet coefficients retained by the algorithm defines an order of magnitude of the memory requirements, in units corresponding to one coefficient per unit of memory, as

$$[M_\mathrm{s}]_{(B,T)}(\alpha) = [R_\mathrm{s}]_{(B,T)}(\alpha) \times \mathcal{O}(B^2). \tag{64}$$

For completeness, let us emphasize that this value accounts for the memory requirements associated with the storage of the wavelet coefficients only. Memory is also required for the storage of the $\mathcal{O}(B^2)$ sampled values $F(\omega_i)$ of the original signal and the $T \times \mathcal{O}(B)$ values of the spherical harmonic coefficients $\widehat{\Psi}_{lm}$ of the continuous wavelet, or equivalently of the spherical harmonic coefficients $\widehat{(\Gamma_{\alpha^j})}_{lm}$ of the scale-discretized wavelets at all analysis depths $j$. Additional temporary memory allocations are also necessary which depend on the precise implementation of the algorithm. Hence, the value $[M_\mathrm{s}]_{(B,T)}(\alpha)$ is to be considered as a lower bound but still fixes an order of magnitude for the memory requirements of the algorithm.

In the extreme case of a large basis dilation factor $\alpha \geq B$, the compact harmonic support of the scale-discretized wavelet essentially gets as large as the band limit, with a compactness $c(\alpha^2) \leq B^2/(B^2 - 1)$. The maximum analysis depth goes to unity, $J_B(\alpha) = 1$, which implies that only two scales are required for the analysis. The storage redundancy reaches its lowest value $[R_\mathrm{s}]_{(B,T)}(\alpha) = 2T$. As soon as $\alpha < B$, the harmonic support of the scale-discretized wavelet obviously gets more compact and more scales are required. For values of the basis dilation factor very close to unity, the compactness gets very high and may prevent the wavelets to be localized enough in real space at the smallest analysis scale. A typically absurd value $\alpha \leq [B/(B - 1)]^{1/2}$ gives $c(\alpha^2) \geq B$, which corresponds to a compact harmonic support selecting at maximum one frequency at a time. This simply reminds us of the fact that too high compactnesses are prohibited in the framework of a wavelet analysis. Let us fix ideas on practical intermediate values of $\alpha < B$. Note that the storage redundancy increases with the band limit $B$, as $J_B(\alpha)$ defined in relation (50) obviously increases with $B$ for a fixed value of $\alpha$. We give the upper bounds in the limit $B \to \infty$ and $J_B(\alpha) \to \infty$. A dyadic decomposition of the scales $\alpha = 2$ corresponds to a compactness $c(4) = 4/3$, and the storage redundancy is bounded by

$[R_\mathrm{s}]_{(B,T)}(2) \leq 7T/3$ for any band limit $B$. A steerability relation with $T = 3$ hence gives a bound $[R_\mathrm{s}]_{(B,T)}(2) \leq 7$. A more compact support of the scale-discretized wavelets set by $\alpha = 1.1$ corresponds to a compactness $c(1.21) \simeq 6$, and the bound on the redundancy rises to $[R_\mathrm{s}]_{(B,T)}(1.1) \lesssim 7T$. A value $T = 3$ then already gives $[R_\mathrm{s}]_{(B,T)}(1.1) \lesssim 21$.

## 5.4 Computation time requirements

We define the *computation redundancy* of the algorithm as the ratio of the number of operations required for the analysis and reconstruction of a signal at all analysis depths with scale-discretized wavelets, to the corresponding number of operations at the first depth ($j = 0$) and per azimuthal frequency ($T = 1$, as for an axisymmetric wavelet which contains only $m = 0$). A low computation redundancy is essential for achieving as low computation time requirements as possible.

The precalculation consists of the computation of the spherical harmonic coefficients $\widehat{(\Gamma_{\alpha^j})}_{lm}$ of the scale-discretized wavelets from a continuous wavelet. At each analysis depth $j$, the computation of the scale-discretized kernel requires a one-dimensional numerical integration of relation (44). The corresponding number of operations required is independent of $\alpha$ as each real value $k \in [1, B)$ is covered exactly once by the continuous wavelets at all analysis depths $j$, whose kernels have compact supports in the intervals $k \in (\alpha^{-(1+j)}B, \alpha^{-j}B)$. The point-wise product between the scale-discretized kernel and the directional split in (40) requires $T \times \mathcal{O}(B)$ operations. As it clearly appears in the following, the cost of these operations is negligible relative to the cost of the analysis and reconstruction themselves. Moreover, it must be performed only once for all signals to be analysed.

The analysis at a single analysis depth $j$ consists in a simple directional correlation of $F$ with $\Gamma_{\alpha^j}$ on S$^2$, leading to the wavelet coefficients on SO(3). The a priori number of operations for a naive quadrature in relation (52) is of the order of $\alpha^{5(1-j)} \times \mathcal{O}(B^5)$, which becomes rapidly unaffordable. Fast directional correlation algorithms based on relation (53) and on the separation of the three variables of integration on SO(3) were recently developed (Wandelt & Górski 2001; Wiaux et al. 2006; McEwen et al. 2007a; Wiaux et al. 2007). They allow for the exact computation of the sampled values $W_\Gamma^F(\rho_{I(j)}, \alpha^j)$ of the wavelet coefficients at each analysis depth $j$ through a number of operations at maximum of the order of $\alpha^{3(1-j)}T \times \mathcal{O}(B^3)$. This number of operations is mainly driven by the Wigner $D$-function transform and naturally scales linearly with the number $M = T$ of rotation angles $\chi_p$ required by the steerability of the wavelet.[3] The reconstruction is symmetric to the analysis and therefore requires the same number of operations, in reverse order. The computation redundancy of the algorithm is thus obtained by accounting for the steerability and summing over all analysis depths $j$ with $0 \leq j \leq J$. In the most exacting case where $J = J_B(\alpha)$, it simply reads as

$$[R_\mathrm{c}]_{(B,T)}(\alpha) = \left[1 + c\left(\alpha^3\right)\left(1 - \alpha^{-3J_B(\alpha)}\right)\right] T. \tag{65}$$

---

[3] For the spherical harmonic transform of the signal, fast algorithms exist on equiangular pixelizations (Driscoll & Healy 1994; Healy et al. 2003, 2004), as well as on Gauss–Legendre (Doroshkevich et al. 2005a,b) and HEALPIX (Górski et al. 2005) pixelizations. The corresponding number of operations required is at maximum of the order of $\alpha^{3(1-j)} \times \mathcal{O}(B^3)$, thanks to the separation of the two variables of integration on S$^2$.

The number of operations required by the algorithm defines an order of magnitude of the computation time requirements, in units corresponding to one operation per unit of time, as

$$[T_c]_{(B,T)}(\alpha) = [R_c]_{(B,T)}(\alpha) \times \mathcal{O}(B^3). \qquad (66)$$

In this expression, the impact of the compact harmonic support of the scale-discretized wavelet is concentrated in $c(\alpha^3) = \alpha^3/(\alpha^3 - 1) \in [1, \infty)$.

Let us again fix ideas on practical intermediate values of $\alpha < B$, and establish upper bounds in the limit $B \to \infty$ and $J_B(\alpha) \to \infty$. A dyadic decomposition of the scales $\alpha = 2$ corresponds to a generalized compactness $c(8) = 8/7$, and the computation redundancy is bounded by $[R_c]_{(B,T)}(2) = 15T/7$ for any band limit $B$. A steerability relation with $T = 3$ hence gives a bound $[R_c]_{(B,T)}(2) \leq 45/7 \simeq 6.5$. A more compact support of the scale-discretized wavelets set by $\alpha = 1.1$ corresponds to a generalized compactness $c(1.331) \simeq 4$, and the bound on the redundancy rises to $[R_c]_{(B,T)}(1.1) \lesssim 5T$. A value $T = 3$ then gives $[R_c]_{(B,T)}(1.1) \lesssim 15$.

## 5.5 Implementation

The proposed algorithm was implemented and tested on a 2.2 GHz Intel Core 2 Duo CPU with 2 Gigabytes of RAM. As already emphasized, the choice of the pixelization on which the original signal $F$ is sampled is essential to ensure the exactness or high precision of the mere computation of its spherical harmonic coefficients and hence of the whole analysis and reconstruction process. The exactness of the proposed algorithm is simply tested by considering that the analysis starts at the level of the spherical harmonic coefficients $\widehat{F}_{lm}$ of the original signal, and ends at the level of the spherical harmonic coefficients $\widehat{\bar{F}}_{lm}$ of the reconstructed signal $\bar{F}$. We also tested the memory and computation time requirements. Let us recall that the corresponding contributions associated with the removed direct spherical harmonic transform of the original signal $F$ and inverse spherical harmonic transform leading to the reconstructed signal $\bar{F}$ are overwhelmed by the inverse and direct Wigner $D$-function transforms required at each analysis depth $j$. Band limits $B \in \{64, 128, 256, 512, 1024\}$ are considered and the basis dilation factor is set to $\alpha = 2$, hence defining a typical dyadic decomposition of scales. At each band limit, five test signals are considered, directly defined through random spherical harmonic coefficients $\widehat{F}_{lm}$ with independent real and imaginary parts uniformly distributed in the interval $(-1, 1)$. The steerable wavelet $\Gamma$ defined and illustrated in Section 4.4 is used, for an azimuthal band limit $N = 3$. It only contains the $T = 3$ even values $m \in \{-2, 0, 2\}$. As discussed in Section 3.1, the basis functions for the steerability can be chosen as the three rotated versions $\Gamma_{\chi_p}$ with $\chi_p = \pi p/3$ for $0 \leq p \leq 2$, and the function $k(\chi)$ follows accordingly. The analysis is performed up to the maximum analysis depth for each band limit: $J_{64}(2) =$

$6, J_{128}(2) = 7, J_{256}(2) = 8, J_{512}(2) = 9$, and $J_{1024}(2) = 10$. The numerical error associated with the algorithm is evaluated as the maximum absolute value, for all values of $l$ and $m$, of the difference between the original and reconstructed spherical harmonic coefficients: $\epsilon = \max_{l,m} |\widehat{F}_{lm} - \widehat{\bar{F}}_{lm}|$. The algorithm is coded with double precision numbers, which sets the unit of memory for the storage of coefficients to 8 bytes.

The memory used $\mu$, as well as computation times $\tau$ and numerical errors $\epsilon$ both averaged over the five random test signals are reported in Table 1. The values reported, respectively, illustrate the memory requirements (64), the computation time requirements (66), and the exactness of reconstruction of the proposed algorithm.

## 6 ASTROPHYSICAL APPLICATION

In this section, we emphasize an important astrophysical application of the wavelet formalism defined and implemented, discussing in some detail the issue of the detection of cosmic strings through the denoising of full-sky CMB data. We first introduce the question of the existence of topological defects in the Universe. We highlight the non-Gaussianity of the component of the CMB signal induced by cosmic strings and justify a wavelet decomposition of the data as a way to enhance the sparsity of the wavelet coefficients of the string signal. We then propose a denoising method based on a statistical model of the wavelet coefficients of the string signal. We also emphasize the need for a precise test allowing one to set a confidence level on the string signal reconstructed from the denoised wavelet coefficients.

### 6.1 Topological defects

Observations of the CMB and of the large-scale structure of the Universe have led to the definition of a concordance cosmological model. The full-sky data of the *WMAP* experiment have played a dominant role in developing this precise picture of the Universe (Bennett et al. 2003; Spergel et al. 2003; Hinshaw et al. 2007; Spergel et al. 2007; Hinshaw et al. 2008; Komatsu et al. 2008). In this framework, the cosmic structures originate largely from Gaussian adiabatic perturbations seeded in the early phase of inflation of the Universe. However, cosmological scenarios motivated in the context of theories unifying the fundamental interactions suggest the existence of topological defects resulting from phase transitions at the end of inflation. These defects would have participated to the formation of the cosmic structures. While textures are more or less axisymmetric, cosmic strings are a line-like version of defects (Turok & Spergel 1990; Vilenkin & Shellard 1994; Hindmarsh & Kibble 1995). Even though observations largely fit

**Table 1.** Test of the implementation of the proposed algorithm for the analysis and reconstruction of signals on the sphere with scale discretized wavelets. Memory used $\mu$ in Megabytes (MB), as well as computation times $\tau$ in minutes (min) and numerical errors $\epsilon$ both averaged over five random test signals are reported, as measured on a 2.2 GHz Intel Core 2 Duo CPU with 2 Gigabytes of RAM. Five band limits are considered $B \in \{64, 128, 256, 512, 1024\}$, and the basis dilation factor is set to $\alpha = 2$. The signals are decomposed up to the maximum analysis depths at each band limit. The steerable wavelet used has an azimuthal band limit $N = 3$, with only the $T = 3$ even values of the azimuthal index allowed: $m \in \{-2, 0, 2\}$.

| $B$ | 64 | 128 | 256 | 512 | 1024 |
|---|---|---|---|---|---|
| $\mu$ (MB) | 1.3 | 5.3 | 21 | 84 | 340 |
| $\tau$ (min) | 0.019 | 0.092 | 0.73 | 7.0 | 72 |
| $\epsilon$ | $8.6 \times 10^{-14}$ | $3.2 \times 10^{-13}$ | $8.9 \times 10^{-13}$ | $2.2 \times 10^{-12}$ | $7.4 \times 10^{-12}$ |

with an origin of the cosmic structures in terms adiabatic perturbations, room is still available for the existence of a small fraction of topological defects. Moreover, fundamental string theory predicts the existence of cosmic strings in the "brane-world" scenario (Davis & Kibble 2005). As a consequence, the issue of the existence of topological defects represents today a central question in cosmology.

Textures would induce hot and cold spots in the CMB with typical angular sizes of several degrees on the celestial sphere (Turok & Spergel 1990). A recent analysis (Cruz et al. 2007) of the *WMAP* data showed that the cold spot detected at $(\theta, \varphi) = (147°, 209°)$ in Galactic spherical coordinates, is satisfactorily described by a texture with an angular size around 10°. The main signature of cosmic strings in the CMB is known as the Kaiser–Stebbins effect (Kaiser & Stebbins 1984), characterized by temperature steps along the strings, with a typical angular size below 1° on the celestial sphere. Constraints have been set on a possible string contribution in terms of upper limits on the so-called string tension $G\mu$, where $G$ stands for the gravitational constant. The string tension sets the overall amplitude of the string contribution. These constraints mainly come from the analysis of the string contribution to the overall CMB angular power spectrum (Contaldi et al. 1999; Wyman et al. 2005, 2006; Bevis et al. 2008). Very few algorithms have been designed for the explicit identification of cosmic strings through the Kaiser–Stebbins effect on full-sky data (Jeong & Smoot 2005; Lo & Wright 2005). No strong detection of cosmic strings has ever been reported.

Current CMB experiments, among which *WMAP*, achieve an angular resolution on the celestial sphere of the order of 10 arcmin, corresponding to a limit frequency $B \simeq 2 \times 10^3$. These experiments constrain a possible string signal to be largely dominated by the standard Gaussian CMB contribution at the frequencies $l$ probed, but it might nevertheless become a dominant contribution at higher frequencies, due to the slow decay of the corresponding angular power spectrum (Fraisse et al. 2007; Bevis et al. 2008). The *Planck* experiment will provide full-sky CMB data at a resolution of 5 arcmin, that is, with $B \simeq 4 \times 10^3$ (Bouchet 2004). Important new information relative to a cosmic string signal will therefore be available.

In this perspective, we sketch in the following a new statistical approach (Wiaux et al. 2008) for the identification and reconstruction of cosmic strings through the denoising of full-sky CMB data. It is specifically considered in the framework of the scale-discretized steerable wavelet formalism on the sphere.[4] Further refinement of this approach, as well as its precise implementation, its application to CMB data, and its comparison with other detection algorithms, are the subjects of a future work.

---

[4] Note that experiments such as the Arcminute Microkelvin Imager (AMI) (Jones 2002; Barker et al. 2006), the Atacama Cosmology Telescope (ACT) (Kosowsky 2006), or the South Pole Telescope (SPT) (Ruhl et al. 2004) will map the CMB at a resolution around 1 arcmin, that is, with $B \simeq 2 \times 10^4$. The corresponding prospects for the detection of strings are thus improved relative to *Planck* data, but these experiments will provide observations of small portions of the celestial sphere only. Specific algorithms for the identification of cosmic strings in CMB data on planar patches must be considered. As a formalism of scale-discretized steerable wavelets also exists on the plane (Simoncelli et al. 1992), it can also be used for the identification and reconstruction of cosmic strings through the denoising of CMB data on planar patches, in a statistical approach analogous to the one proposed below (Wiaux et al. 2008).

## 6.2 Non-Gaussian string signal

The standard component of the CMB signal induced by adiabatic perturbations is a Gaussian signal on the sphere with a known angular power spectrum in a given cosmological model. Topological defects and, in particular, cosmic strings, induce a non-Gaussian component of the CMB signal with characteristic features defined at specific positions and scales. The corresponding angular power spectrum exhibits a fixed characteristic shape, with a slow decay at high frequencies. The complete non-Gaussian statistical distribution of a string signal and the corresponding angular power spectrum can indeed be deduced from simulations in the chosen cosmological model (Fraisse et al. 2007; Bevis et al. 2008), up to an overall amplitude of the string contribution as set by the unknown string tension $G\mu$. These two statistically independent components simply add linearly. We consider the perturbations of the signals around their statistical mean. Instrumental Gaussian white noise with zero mean also unavoidably adds as an independent component, setting the limited sensitivity of the experiment considered. We leave apart any issue of deconvolution of the experimental beam and also discard problems of contamination of CMB data by foreground emissions. In the perspective of the detection of cosmic strings, the non-Gaussian component from strings represents the signal to be identified and reconstructed, while the Gaussian components can be seen as a statistically independent Gaussian noise. The overall signal $F$ reads as the sum of the string signal and the noise in terms of a linear combination

$$F(\omega_i) = a_s F_s(\omega_i) + F_n(\omega_i), \qquad (67)$$

where $F_s$ represents the string signal for a string tension $a_s = G\mu$ normalized to unity, and $F_n$ represents the noise. The zero mean signals $F$, $F_s$ and $F_n$ are considered to have a band limit $B$, related to the resolution of the experiment under consideration, and a number $\mathcal{O}(B^2)$ of points $\omega_i$ are required for their precise description.

In the first approximation, we can fix the cosmological parameters at their values in the concordance cosmological model. This fixes the angular power spectra of the noise $F_n$ and of the normalized string signal $F_s$.

## 6.3 Sparse wavelet coefficients

Wavelets are by construction filters with zero mean (see (48)). As such, they generically enhance discontinuities, and reduce smooth patterns in the signal analysed. The non-Gaussian string signal characterized by temperature steps typically has a sparse expansion in terms of wavelets. It indeed only exhibits a small number of wavelet coefficients of large absolute value at the specific positions of the strings and at their characteristic scales. On the contrary, the Gaussian contributions are characterized by smooth patterns designed by their angular correlation functions. Their expansion in terms of wavelets is not sparse. The sparsity of the wavelet coefficients of the string signal justifies the wavelet decomposition of the data. Moreover, directional wavelets (i.e. with an azimuthal band limit $N > 1$) particularly apply for an efficient detection of the localized directional features associated with the Kaiser–Stebbins effect. Indeed, the more similar the filter to the signal signatures, the better it magnifies these signatures. Correspondingly, the detection of textures would more naturally follow from an analysis with axisymmetric wavelets ($N = 1$). Finally, as emphasized already, the scale discretization of the wavelets is essential for the reconstruction of the signal. In conclusion, the denoising procedure will be more efficient

when applied to the wavelet coefficients of the signal observed $F$ decomposed with a scale-discretized steerable wavelet.

A suitable scale-discretized steerable wavelet $\Gamma$ is thus chosen with a given directionality set in terms of an azimuthal band limit $N$. The basis dilation factor $\alpha$ and the total analysis depth $J$ are also chosen, in order to optimize the number of analysis depths in the range of frequencies $l$ concerned by the string signal. Let us recall that the sampling of the wavelet coefficients of a signal is defined on the points $\rho_{I(j)} = ((\omega_0)_{i(j)}, \chi_p)$ on SO(3). The value $I(j) = \{i(j), p\}$ simply indexes these points at each analysis depth $j$ with $0 \leq j \leq J \leq J_B(\alpha)$. They correspond to the points $(\omega_0)_{i(j)}$ on S$^2$ for each value of the rotation angle $\chi_p$, with $0 \leq p \leq T - 1$, as required by the steerability (see Section 5.1). By linearity of the wavelet decomposition (52), the wavelet coefficients $W_\Gamma^F$ of the overall signal $F$ read, in terms of the wavelet coefficients of the normalized string signal $F_s$ and of the noise $F_n$, as

$$W_\Gamma^F \left( \rho_{I(j)}, \alpha^j \right) = a_s W_\Gamma^{F_s} \left( \rho_{I(j)}, \alpha^j \right) + W_\Gamma^{F_n} \left( \rho_{I(j)}, \alpha^j \right), \qquad (68)$$

with $a_s W_\Gamma^{F_s} = W_\Gamma^{a_s F_s}$. The wavelet coefficients $W_\Gamma^F$, $W_\Gamma^{F_s}$ and $W_\Gamma^{F_n}$ have zero statistical means just as the corresponding signals.

## 6.4 Statistical model

In a training phase, the statistical distributions of the wavelet coefficients of a pure noise $F_n$ and of a pure normalized string signal $F_s$ must be identified.

For the noise $F_n$, the wavelet coefficients remain Gaussian by linearity. Assuming the statistical isotropy of the noise, the probability density functions of the zero mean wavelet coefficients $W_\Gamma^{F_n}$ depend on the analysis depth $j$ but are independent of $\rho_{I(j)}$:

$$f_j^{F_n} \left( W_\Gamma^{F_n} \right) \sim \exp \left[ -\frac{1}{2} \left( \frac{W_\Gamma^{F_n}}{\sigma_j^{F_n}} \right)^2 \right]. \qquad (69)$$

The variances $(\sigma_j^{F_n})^2$ can be inferred from the known angular power spectrum of the noise in the range of frequencies probed by the wavelets at the different analysis depths.

For the normalized string signal $F_s$, a Monte Carlo analysis based on string signal simulations (Fraisse et al. 2007; Bevis et al. 2008) is required to fit a non-Gaussian model of the probability density function at each depth $j$. The more reliable the simulations, the better the model for the probability density functions. As a first approximation, the computation of the variance and kurtosis of the wavelet coefficients allows one to fit a generalized Gaussian distribution at each depth. Assuming the statistical isotropy of the string signal, the probability density functions of the zero mean wavelet coefficients $W_\Gamma^{F_s}$ again depend on the analysis depth $j$ but are independent of $\rho_{I(j)}$:

$$f_j^{F_s} \left( W_\Gamma^{F_s} \right) \sim \exp \left( -\left| \frac{W_\Gamma^{F_s}}{u_j} \right|^{h_j} \right). \qquad (70)$$

The parameters $u_j$ relate to the standard deviations $\sigma_j^{F_s}$ of the distributions. The corresponding variances $(\sigma_j^{F_s})^2$ reflect the angular power spectrum of the string signal in the range of frequencies probed by the wavelets at the different analysis depths. The parameters $h_j$ obviously measure the peakedness of the distributions, and relate to their kurtoses. At the analysis depths corresponding to the characteristic range of frequencies concerned by the string signal, the sparsity of the wavelet coefficients can be associated with peaked distributions $f_j^{F_s}$ with heavy tails (*i.e.* with kurtoses larger than 3, or values $0 < h_j < 2$) relative to a Gaussian distribution (*i.e.* with a kurtosis equal to 3, or a value $h_{\text{Gaussian}} = 2$).

## 6.5 Denoising

The identification and reconstruction of a string signal from real data can then be implemented as follows.

First, the overall signal $F$ is decomposed with the chosen scale-discretized steerable wavelet $\Gamma$, which gives the wavelet coefficients $W_\Gamma^F$ through relation (52).

Secondly, the string tension associated with a still hypothetical string signal is estimated in relation (67). A precise approach based on the analysis of the angular power spectrum of the real data could be adopted, consisting in a likelihood analysis involving all cosmological parameters including the string tension. This standard approach was used to obtain the current constraints on the string tension (Bevis et al. 2008), together with a reassessment of the other cosmological parameters. The distributions $f_j^{F_n}$ and $f_j^{F_s}$ should then also be reassessed according to the modified angular power spectra for $F_n$ and $F_s$, respectively. However, in the approximation considered, all cosmological parameters are fixed at their values in the concordance cosmological model throughout the analysis. The angular power spectra of the noise $F_n$ and of the normalized string signal $F_s$ are thus kept invariant. A rough estimation of the string tension $a_s = G\mu$ is obtained from a least-squares method based on the variances of the wavelet coefficients of $F$, $F_s$, and $F_n$ at all depths $j$. It is primarily intended to serve the denoising itself and not as a final estimation of the string tension. The wavelet decomposition here simply helps to bin the values of the power spectra before defining the constraints. By statistical independence, the variances $(\sigma_j^F)^2$ of the overall signal $F$ at each depth $j$ read, in terms of the variances $(\sigma_j^{F_s})^2$ of the normalized string signal $F_s$ and of the variances $(\sigma_j^{F_n})^2$ of the noise $F_n$, as

$$\left( \sigma_j^F \right)^2 = a_s^2 \left( \sigma_j^{F_s} \right)^2 + \left( \sigma_j^{F_n} \right)^2, \qquad (71)$$

with $a_s^2(\sigma_j^{F_s})^2 = (\sigma_j^{a_s F_s})^2$. The wavelet coefficients $W_\Gamma^F$ are thus assumed to satisfy relation (68) for an estimation $\bar{a}_s$ of the exact value $a_s$. The statistical distributions $f_j^{F_n}$ for the wavelet coefficients $W_\Gamma^{F_n}$ of the noise $F_n$ are identified as in relation (69). The statistical distributions $f_j^{\bar{a}_s F_s}$ for the wavelet coefficients $W_\Gamma^{\bar{a}_s F_s}$ of the string signal $\bar{a}_s F_s$ are as in relation (70) with $u_j \rightarrow \bar{a}_s u_j$ and $h_j$ is left invariant. By Bayes' theorem, the posterior probability distribution function $f_j^{(\bar{a}_s F_s | F)}$ at each depth $j$ for the wavelet coefficients $W_\Gamma^{\bar{a}_s F_s}$, given the observed values $W_\Gamma^F$, reads as

$$f_j^{(\bar{a}_s F_s | F)} \left( W_\Gamma^{\bar{a}_s F_s} | W_\Gamma^F \right) \sim f_j^{F_n} \left( W_\Gamma^F - W_\Gamma^{\bar{a}_s F_s} \right)$$
$$\times f_j^{\bar{a}_s F_s} \left( W_\Gamma^{\bar{a}_s F_s} \right). \qquad (72)$$

Note that one could also easily account for a flexibility in the overall amplitude of the standard Gaussian component of the CMB, associated with the cosmological parameter $\sigma_8$, in the same least-squares approach.

Thirdly, from the identified posterior probability, the wavelet coefficients $W_\Gamma^{a_s F_s}$ of the string signal are estimated to values $\bar{W}_\Gamma^{a_s F_s}$, separately at each point $\rho_{I(j)}$ for each analysis depth $j$. For example, in a maximum a posteriori approach, this estimation is defined as the value which maximizes the posterior probability, while in a Bayesian least square approach, it is defined as the expectation value of the posterior probability.

Finally, the estimated string signal $\overline{a_s F_s}$ is reconstructed from the denoised wavelet coefficients $\bar{W}_\Gamma^{a_s F_s}$ through relations (54) and (55). The string network imprinted in the analysed CMB data is readily mapped as the magnitude of gradient of the reconstructed signal.

## 6.6 Confidence level of detection

For the reasons discussed above, scale-discretized steerable wavelets should represent a very powerful tool for the identification and the reconstruction of the string signal buried in the standard Gaussian component of the CMB and in instrumental noise. The statistical approach considered for the denoising procedure at each point $\rho_{I(j)}$ for each analysis depth $j$ specifically accounts for the shape of the power spectra of the string signal and of the Gaussian components. It also accounts for the peakedness of the non-Gaussian string signal, characterized by a large kurtosis at each analysis depth $j$ characteristic of the string signal.

After reconstruction, a hypothesis test can be set up in order to assess if the estimated string network indeed arises from a string signal with high probability. For example, the kurtosis of the magnitude of gradient of the reconstructed signal can be compared to the corresponding reconstructed kurtosis of combinations (67) of a string signal with noise, through Monte Carlo analyses for various string tensions. More statistics may also be combined, such as the variances and kurtoses at different resolutions of the magnitude of gradient of the reconstructed signal, in order to provide a more robust hypothesis test. This procedure is also intended to provide a estimation of the string tension $a_s = G\mu$ from the denoised signal, more precise than the original estimation $\bar{a}_s$ which first served to the denoising.

Let us finally notice that the Canny algorithm (Canny 1986) was recently proposed for the detection of cosmic strings in CMB data on planar patches (Amsel et al. 2007). It consists of an edge detection in the map of the magnitude of gradient of the original signal, independently of any denoising approach. This method could be implemented for the analysis of full-sky CMB data, and compared to our algorithm in order to assess their relative performances. In the context of our denoising approach, this edge detection might actually be applied to the magnitude of gradient of the denoised signal, in order to count the string segments obtained, instead of computing the corresponding kurtosis. The confidence level of the detection could then be assessed by comparison with the corresponding counts for pure noise through a Monte Carlo analysis.

## 7 CONCLUSION

We have derived a scale-discretized wavelet formalism for the analysis and exact reconstruction of band-limited signals on the sphere with directional wavelets. The combination of the two properties of exact reconstruction and directionality was lacking in the existing wavelet formalisms. As for the formalism developed by Antoine & Vandergheynst (1999) and Wiaux et al. (2005), the translations of the wavelets at any point on the sphere and their proper rotations are still defined through the continuous three-dimensional rotations. However, the wavelets are factorized steerable functions with compact harmonic support, and they are dilated through a kernel dilation directly defined in harmonic space.

As an intermediate step, a continuous wavelet formalism was obtained. This by-product of our developments can be understood as an alternative approach for the analysis of signals, with wavelets bearing new compact harmonic support and directionality properties. However, the continuous range of scales required for the analysis still prevents in practice the exact reconstruction of the signals analysed from their wavelet coefficients.

The scale-discretized wavelet formalism results from an integration by slices of the dilation factor of the continuous formalism. It allows in practice the exact reconstruction of band-limited signals from their wavelet coefficients with a finite number of scales. It can also be derived independently of the continuous wavelets, and can be understood as a generalization of existing invertible filter bank methods. The multi-resolution properties of the formalism were identified and a corresponding exact algorithm was described. The memory and computation time requirements were discussed and an implementation was tested.

This formalism is of interest in a large variety of fields, notably for the denoising or the deconvolution of signals on the sphere with a sparse expansion in wavelets. It typically concerns signals identified by directional features at specific positions and scales. In astrophysics, it finds a particular application for the identification of localized directional features in CMB data, such as the imprint of topological defects, in particular, cosmic strings, and for their reconstruction after separation from the other signal components. In this context, we have discussed a new statistical approach for the detection of cosmic strings through the denoising of full-sky CMB data. This application is the subject of a future work.

## REFERENCES

Abramowitz M., Stegun I., 1965, Handbook of mathematical functions. Dover Publications Inc., New York
Amsel S., Berger J., Brandenberger R. H., 2007, preprint (arXiv:0709.0982)
Antoine J.-P., Vandergheynst P., 1998, J. Math. Phys., 39, 3987
Antoine J.-P., Vandergheynst P., 1999, Appl. Comput. Harm. Anal., 7, 262
Antoine J.-P., Vandergheynst P., 2007, J. Fourier Anal. Applic., 13, 369
Antoine J.-P., Demanet L., Jacques L., Vandergheynst P., 2002, Appl. Comput. Harm. Anal., 13, 177
Antoine J.-P., Murenzi R., Vandergheynst P., Ali S. T., 2004, Two-dimensional Wavelets and their Relatives. Cambridge Univ. Press, Cambridge
Baldi P., Kerkyacharian G., Marinucci D., Picard D., 2006, preprint (math/0606599)
Barker R. et al., 2006, MNRAS, 369, L1
Bennett C. L. et al., 2003, ApJS, 148, 1
Bevis N., Hindmarsh M., Kunz M., Urrestilla J., 2008, Phys. Rev. Lett., 100, 021301
Bogdanova I., Vandergheynst P., Antoine J.-P., Jacques L., Morvidone M., 2005, Appl. Comput. Harm. Anal., 19, 223
Bouchet F. R., 2004, preprint (astro-ph/0401108)
Brink D. M., Satchler G. R., 1993, Angular Momentum, 3rd edn. Clarendon Press, Oxford
Canny J., 1986, IEEE Trans. Pattern Anal. Machine Intell., 8, 679
Contaldi C., Hindmarsh M., Magueijo J., 1999, Phys. Rev. Lett., 82, 679
Cruz M., Turok N., Vielva P., Martínez-González E., Hobson M. P., 2007, Sci, 318, 1612
Daubechies I., Defrise M., Demol C., 2004, Comm. Pure Appl. Math., LVII, 1413
Davis A. C., Kibble T. W. B., 2005, Contemp. Phys., 46, 313
Demanet L., Vandergheynst P., 2003, in Unser M. A., Aldroubi A., Laine A. F., eds, Proc. SPIE Vol. 5207, Wavelets: Applications in Signal and Image Processing X. SPIE, Bellingham, p. 208
Doroshkevich A. G., Naselsky P. D., Verkhodanov O. V., Novikov D. I., Turchaninov V. I., Novikov I. D., Christensen P. R., Chiang L.-Y., 2005a, Int. J. Mod. Phys. D, 14, 275

Doroshkevich A. G., Naselsky P. D., Verkhodanov O. V., Novikov D. I., Turchaninov V. I., Novikov I. D., Christensen P. R., Chiang L.-Y., 2005b, preprint (astro-ph/0501494)

Driscoll J. R., Healy D. M., Jr, 1994, Adv. Appl. Math., 15, 202

Duval-Destin M., Muschietti M. A., Torrésani B., 1993, SIAM J. Math. Anal., 24, 739

Fraisse A. A., Ringeval C., Spergel D. N., Bouchet F. R., 2007, preprint (arXiv:0708.1162)

Frazier M., Jawerth B., Weiss G., 1991, CMBS Regional Conference Series in Mathematics Vol. 79, Littlewood-Paley Theory and the Study of Function Spaces. American Math. Soc.

Freeden W., Windheuser U., 1996, Adv. Comput. Math., 5, 51

Freeden W., Gervens T., Schreiner M., 1998, Constructive Approximation on the Sphere, with Applications to Geomathematics. Clarendon Press, Oxford

Freeman W. T., Adelson E. H., 1991, IEEE Trans. Pattern Anal. Machine Intell., 13, 891

Górski K. M., Hivon E., Banday A. J., Wandelt B. D., Hansen F. K., Reinecke M., Bartelman M., 2005, Astrophys. J., 622, 759

Guilloux F., Faÿ G., Cardoso J.-F., 2007, preprint (arXiv:0706.2598)

Healy D. M., Jr, Rockmore D. N., Kostelec P. J., Moore S., 2003, J. Fourier Anal. Applic., 9, 341

Healy D. M., Jr, Kostelec P. J., Rockmore D. N., 2004, Adv. Comput. Math., 21, 59

Hindmarsh M., Kibble T. W. B., 1995, Rep. Prog. Phys., 58, 477

Hinshaw G. et al., 2007, ApJS, 170, 288

Hinshaw G. et al., 2008, preprint (arXiv:0803.0732)

Holschneider M., 1996, J. Math. Phys., 37, 8

Jeong E., Smoot G. F., 2005, ApJ, 624, 21

Jones M. E., 2002, in Chen L.-W., Ma C.-P., Ng K.-W., Pen U.-L., eds, ASP Conf. Ser. Vol. 257, AMiBA 2001: High-z Clusters, Missing Baryons, and CMB Polarization. Astron. Soc. Pac., San Francisco, p. 35

Kaiser N., Stebbins A., 1984, Nat, 310, 391

Komatsu E. et al., 2008, ApJS, submitted (arXiv:0803.0547)

Kosowsky A., 2006, New Astron. Rev., 50, 969

Kostelec P. J., Rockmore D. N., 2003, Technical report (SFI-03-11-060)

Lo A. S., Wright E. L., 2005, preprint (astro-ph/0503120)

Mallat S., 1998, A Wavelet Tour of Signal Processing. Academic Press, San Diego

Marinucci D. et al., 2007, preprint (arXiv:0707.0844)

Maslen D. K., Rockmore D. N., 1997a, J. American Math. Soc., 10, 169

Maslen D. K., Rockmore D. N., 1997b, in Finkelstein L., Kantor, W., eds, Proc. DIMACS Workshop on Groups and Computation 28. American Math. Soc., Providence, p. 183

McEwen J. D., Hobson M. P., Lasenby A. N., 2006, preprint (astro-ph/0609159)

McEwen J. D., Hobson M. P., Mortlock D. J., Lasenby A. N., 2007a, IEEE Trans. Signal Proc., 55, 520

McEwen J. D. et al., 2007b, J. Fourier Anal. Applic., 13, 495

Muschietti M. A., Torrésani B., 1995, SIAM J. Math. Anal., 26, 925

Narcowich F. J., Petrushev P., Ward J. D., 2006, SIAM J. Math. Anal., 38, 574

Ruhl J. E. et al., 2004, in Zmuidzinas J., Holland W. S., Withington S., eds, Proc. SPIE Vol. 5498, Millimeter and Submillimeter Detectors for Astronomy II. SPIE, Bellingham, p. 11

Simoncelli E. P., Freeman W. T., Adelson E. H., Heeger D. J., 1992, IEEE Trans. Information Theo., 38, 587

Spergel D. N. et al., 2003, ApJS, 148, 175

Spergel D. N. et al., 2007, ApJS, 170, 377

Starck J.-L., Murtagh F., 2006a, Astronomical Image and Data Analysis, 2nd edn. Springer, Berlin

Starck J.-L., Moudden Y., Abrial P., Nguyen M., 2006b, A&A, 446, 1191

Turok N., Spergel D. N., 1990, Phys. Rev. Lett. 64, 2736

Vandergheynst P., Gobbers J.-F., 2002, IEEE Trans. Image Proc., 11, 363

Varshalovich D. A., Moskalev A. N., Khersonskii V. K., 1989, Quantum Theory of Angular Momentum (First Edition Reprint). World Scientific Press, Singapore

Vilenkin A., Shellard E. P. S., 1994, Cosmic Strings and Other Topological Defects. Cambridge Univ. Press, Cambridge

Wandelt B. D., Górski K. M., 2001, Phys. Rev. D, 63, 123002

Wiaux Y., Jacques L., Vandergheynst P., 2005, ApJ, 632, 15

Wiaux Y., Jacques L., Vielva P., Vandergheynst P., 2006, ApJ, 652, 820

Wiaux Y., McEwen J. D., Vielva P., 2007, J. Fourier Anal. Applic., 13, 477

Wiaux Y., Hammond D. K., Vandergheynst P., 2008, Technical report (EPFL-LTS-06.2008)

Wyman M., Pogosian L., Wasserman I., 2005, Phys. Rev. D, 72, 023513

Wyman M., Pogosian L., Wasserman I., 2006, Phys. Rev. D, 73, 089905(E)

Yeo B. T. T., Ou W., Golland P., 2006, in Proc. Ieee Int. Conf. Image Proc. (Icip), p. 2161

This paper has been typeset from a TEX/LATEX file prepared by the author.